

This is the peer reviewed version of the following article:

Channelization of a large Alpine River: what is left of its original morphodynamic? / Scorpio, V; Zen, S; Bertoldi, W; Surian, N; Mastrorunzio, M; Dai Prá, E; Zolezzi, G; Comiti, F. - In: EARTH SURFACE PROCESSES AND LANDFORMS. - ISSN 1096-9837. - 43:5(2018), pp. 1044-1062. [10.1002/esp.4303]

Terms of use:

The terms and conditions for the reuse of this version of the manuscript are specified in the publishing policy. For all terms of use and more information see the publisher's website.

03/05/2026 05:59

CHANNELIZATION OF A LARGE ALPINE RIVER: WHAT IS LEFT OF ITS ORIGINAL MORPHODYNAMICS?

Journal:	<i>Earth Surface Processes and Landforms</i>
Manuscript ID	ESP-16-0446.R2
Wiley - Manuscript type:	Research Article
Date Submitted by the Author:	30-Oct-2017
Complete List of Authors:	Scorpio, Vittoria; Free University of Bozano-Bozen, faculty of Science and Technology Zen, Simone; University of Trento, Department of Civil, Environmental and Mechanical Engineering Bertoldi, Walter; University of Trento, Department of Civil, Environmental and Mechanical Engineering Surian, Nicola; University of Padua, Geosciences Marco, Mastrunzio; University of Trento, Department of Humanities Dai Prá, Elena; University of Trento, Department of Humanities Guido, Zolezzi; University of Trento, Department of Civil, Environmental and Mechanical Engineering Comiti, Francesco; Free University of Bolzano, Faculty of Science and Technology
Keywords:	evolutionary trajectories, historical mapping, river channelization, bar theory, Alpine rivers

SCHOLARONE™
Manuscripts



1
2
3 1 **CHANNELIZATION OF A LARGE ALPINE RIVER: WHAT IS LEFT OF ITS**
4
5 2 **ORIGINAL MORPHODYNAMICS?**
6
7
8
9

10 4 Vittoria Scorpio^{1*}, Simone Zen², Walter Bertoldi², Nicola Surian³, Marco Mastronunzio⁴, Elena
11
12 5 Dai Prá⁴, Guido Zolezzi², Francesco Comiti¹
13
14
15
16

17 7 ¹ Faculty of Science and Technology, Free University of Bozen-Bolzano, Bolzano, Italy

18 8 ² Department of Civil, Environmental and Mechanical Engineering, University of Trento, Italy

19 9 ³ Department of Geosciences, University of Padova, Padova, Italy

20 10 ⁴ Department of Humanities, University of Trento, Trento, Italy
21
22
23
24
25
26
27
28

29 12 * Correspondence to: Vittoria Scorpio, Faculty of Science and Technology, Free University of
30
31 13 Bozen-Bolzano, Piazza Università 5, 39100 Bolzano, Italy. E-mail: vittoria.scorpio@unibz.it
32
33
34
35
36
37
38

39 16 **Abstract**

40
41 17 The Adige River drains 12,200 km² of the Eastern Alps and flows for 213 km within this
42
43 18 mountain range. Similarly to other large rivers in Central Europe, the Adige River was subject to
44
45 19 massive channelization works during the 19th century. Thanks to the availability of several
46
47 20 historical maps, this river represents a very valuable case study to document to what extent the
48
49 21 morphology of the river changed due to channelization and understand how much is left of its
50
51 22 original morphodynamics. The study was based on the analysis of 7 sets of historical maps
52
53 23 dating from 1803-1805 to 1915-1927, on geomorphological analysis, on the application of
54
55
56
57
58
59
60

1
2
3 24 mathematical morphodynamic theories and on the application of bar and channel pattern
4
5
6 25 prediction models. The study concerns 115 km of the main stem and 29 km of its tributaries. In
7
8 26 the pre-channelization conditions, the Adige River presented a prevalence of single-thread
9
10 27 channel planform. Multi-thread patterns developed only immediately downstream of the main
11
12 28 confluences. During the 19th century, the Adige underwent considerable channel adjustment,
13
14
15 29 consisting of channel narrowing, straightening, and reduction of bars and islands. Multi-thread
16
17 30 and single-thread reaches evolved through different evolutionary trajectories, considering both
18
19
20 31 the channel width and the bar/vegetation interaction. Bar and channel pattern predictors showed
21
22 32 a good correspondence with the observed patterns, including the development of multi-thread
23
24 33 morphologies downstream of the confluences. Application of the free-bar predictor helped to
25
26
27 34 interpret the strong reduction – almost complete loss – of exposed sediment bars after the
28
29 35 channelization works, quantifying the riverbed inclination to form alternate bars. This
30
31 36 morphological evolution can be observed in other, Alpine rivers of similar size and similar
32
33
34 37 massive channelization, therefore, a simplified model for large rivers subjected to channelization
35
36 38 is proposed, showing that a relatively small difference in the engineered channel width may have
37
38
39 39 a strong impact on the river dynamics, specifically on bar formation.
40
41
42

43
44 41 *Keywords:* evolutionary trajectories, historical mapping, river channelization, bar theory, channel
45
46 42 pattern predictor, Alpine rivers.
47
48
49
50
51
52
53
54
55
56
57
58
59
60

47 **Introduction**

48 Study of historical evolution of river channels has been a central theme in geomorphology for
49 decades (Petts, 1989; Wyzga, 1993; Surian and Rinaldi, 2003; Liébault and Piégay, 2002; Surian
50 et al., 2009a; Scorpio et al., 2015; David et al., 2016). Most studies, at both Italian and European
51 level, have addressed reaches characterized by originally wide braided morphology, while
52 studies analyzing rivers with original single-thread or anastomosed morphologies are very few,
53 i.e. the Rhine River (VanUrk and Smit, 1989, Frings et al., 2011) and Po River (Marchetti,
54 2002). Even analyses performed on large Alpine river systems (Surian et al., 2009a; Comiti et
55 al., 2011; Ziliani and Surian, 2012) have focused especially on reaches with a predominantly
56 braided morphology, excluding the work by Campana et al. (2014).

57 Most recent studies have shown that a sound understanding of channel evolution may be
58 obtained by coupling the reconstruction of evolutionary trajectory of channel morphology with
59 the analysis of driving factors (Ziliani and Surian, 2012; Scorpio and Roskopf, 2016).

60 Channelization has been a major driver of channel adjustments. In Europe, channelization has
61 been planned since the 18th century, fixing new channel widths to satisfy the need of ensuring
62 river navigation, flood protection and increasing the sediment transport capacity (Vischer, 1989;
63 VanUrk and Smit, 1998; Vautier, 2000; Hohensinner et al., 2004; Zawiejska and Wyzga, 2010;
64 Klosch and Habersack, 2016). Most common effects of channelization are channel narrowing,
65 bed-level lowering, and simplification of channel morphology (e.g. from multithread to single
66 thread channel) (Hohensinner et al., 2004; Zawiejska and Wyzga, 2010), but aggradation has
67 been documented in some cases (Siviglia et al., 2008; Davies et al., 2013).

68 Existing studies suggest that (i) predicting morphological effects of channelization in gravel-bed
69 rivers is not straightforward and (ii) channel width is a key parameter controlling river

1
2
3 70 morphodynamics (Garcia Lugo et al., 2015). Nonetheless, the extent to which channelization
4
5
6 71 may modify channel morphodynamics (e.g. bar formation and channel pattern) is still not well
7
8 72 documented.

9
10 73 Also most Alpine rivers were largely modified by human interventions starting from the 19th
11
12 74 century (Wohl, 2006), to ensure flood protection, reclaim agricultural land, and to facilitate
13
14 75 transportation of goods. Direct modification of the river morphology through embankments,
15
16
17 76 planform straightening, sediment mining and dam construction produced notable channel
18
19 77 adjustments in Alpine rivers (Surian et al., 2009a; Comiti, 2012; Ziliani and Surian, 2012;
20
21 78 Campana et al., 2014). Land use and climate change in the catchment further impacted on
22
23 79 sediment production and flow regimes and, therefore, on channel morphology (Bravard, 1989;
24
25
26 80 Liébault and Piégay, 2002; Arnaud-Fassetta, 2003).

27
28
29 81 The Adige River (Eastern Alps, Italy) represents a suitable case study to address the effect of
30
31 82 channelization on channel morphology in mountain fluvial systems. This river was subject to
32
33 83 massive channelization works by the Austrian Administration (under the Habsburg Empire)
34
35 84 during the 19th century. Thanks to the availability of several large scale historical maps it was
36
37 85 possible to analyze channel planform characteristics before channelization and to reconstruct
38
39 86 channel adjustments during and after channelization. The main aims of this study are: (i) to
40
41 87 document to what extent the morphology of the river has changed due to channelization; (ii) to
42
43 88 understand how much is left of its original morphodynamics and iii) to gain insight in the
44
45 89 physical processes controlling the channel changes. To achieve these objectives, the results from
46
47 90 the historical analysis were compared to the estimates of an analytical model (Colombini et al.,
48
49 91 1987) and of two channel pattern predictors (Crosato and Mosselman, 2009; Eaton et al., 2010).
50
51 92 Additionally, a practical outcome of this study is to inform river managers about the possible
52
53
54
55
56
57
58
59
60

1
2
3 93 trajectories of this river, for instance if a restoration project (e.g. channel widening of different
4
5 94 magnitude) were carried out.
6
7

8 95

9
10 96

11
12
13 97 **Study area**

14
15 98 The Adige River (*Etsch* in German) is the second longest river in Italy, with a total length of
16
17 99 approximately 410 km, flowing from the Central-Eastern Alps to the Adriatic Sea. The
18
19
20 100 catchment has an area of about 12,200 km², a maximum elevation of 3905 m a.s.l. (Ortler/Ortles
21
22 101 massif), and it is mainly composed of metamorphic (Alpine Paleozoic basement, mostly gneiss
23
24 102 and micaschists) and volcanic (porphyric) rocks in the upper part, and of sedimentary rocks
25
26
27 103 (especially limestone and dolomites) in the medium part.
28

29 104 The basin hosts 185 glaciers covering currently a total surface of about 130 km², approximately
30
31 105 1% of the total area, but about 6.5% at the upstream end of the study reach, which impart nivo-
32
33
34 106 glacial characteristics to the flow regime of its upper reaches and tributaries. Along the entire
35
36 107 course of the river, minimum flows occur in winter and large floods typically in autumn
37
38 108 associated with long-lasting cyclonic fronts. The mean annual precipitation in the Adige basin
39
40 109 ranges between 400 and 900 mm (Adler et al., 2015), and the mean annual discharge at the outlet
41
42 110 into the sea is 235 m³/s.
43
44

45
46 111 During the Little Ice Age (the peak of which occurred around the middle 19th century (Grove,
47
48 112 2004), Alpine glaciers reached their maximum extension ever reached after the Last Glacial
49
50 113 Maximum. Afterward, they started to decrease in area and volume as a consequence of the
51
52 114 progressive global warming (Fischer et al., 2015). In South Tyrol (the upper Adige catchment),
53
54
55
56
57
58
59
60

1
2
3 115 the loss of glacier area was 376 km², between the Little Ice Age and 1969, corresponding to an
4
5
6 116 area loss of about 40% (Fischer et al., 2015).

7
8 117 An analysis carried out on precipitation variability in Northern Italy indicates a general drying
9
10 118 trend from the wet early 19th century to the dry mid-20th century (Brunetti et al., 2000; 2001;
11
12 119 2006). Afterward, until the early 2010s, precipitations slightly increased, but data do not show
13
14 120 prominent and long-lasting trends (Brunetti et al., 2006).

15
16
17 121 Remarkably, the average slope of the Adige River segment flowing within the Alpine range is
18
19 122 quite lower compared to other rivers of the Eastern Italian Alps (Brenta, Piave, Tagliamento),
20
21 123 most likely as it crosses this mountain range along its wider section. Also, compared to other
22
23 124 large river systems of the Alps, the Adige features an anomalous longitudinal profile, likely
24
25 125 because of the presence of several knickpoints (Robl et al., 2008), and valley widths are large (1-
26
27 126 2 km), likely due to the strong carving action of Quaternary glaciers (Fuganti et al., 1996;
28
29 127 Bassetti and Borsato, 2005).

30
31
32 128 The Adige River has been subjected to a strong channelization and reduction of the river bed
33
34 129 area. Small-scale land reclamation and channel bank works were already carried out in the
35
36 130 Middle Age. However, they were limited to discontinuous portions of banks close to the human
37
38 131 settlements, and they were mostly made of wood and fagots (Autorità di Bacino dell'Adige,
39
40 132 1995). A massive channelization scheme aiming at land reclamation and flood hazard mitigation
41
42 133 was planned since the mid-18th century, and implemented starting from the first decades of the
43
44 134 19th century. Most of the channelization works took place between the 1820s and the 1880s, and
45
46 135 especially following a major flood that hit the entire basin in 1882. Indeed, the Adige River can
47
48 136 be nowadays considered one of the most altered rivers in Italy, not only due to channelization but
49
50 137 also to the presence of many hydropower reservoirs and check-dams along its tributaries that
51
52
53
54
55
56
57
58
59
60

1
2
3 138 make both flow and sediment regimes highly modified (Zolezzi et al., 2009, Chiogna et al.,
4
5
6 139 2016). It is relevant to point out that hydropower dams as well as check-dams for sediment
7
8 140 trapping were mostly built after 1930s-1940s, i.e. after the period considered in this paper (i.e.
9
10 141 1800s-1920s).
11

12
13 142
14
15 143 The valley segment analyzed in this paper extends from the city of Meran/Merano (Autonomous
16
17 144 Province of Bolzano/South Tyrol) to the village of Calliano (Autonomous Province of Trento),
18
19
20 145 for a total length of about 115 km (Figure 1), and with the elevation ranging from 295 m to 170
21
22 146 m a.s.l. Catchment area increases from 2,000 km² at the upstream end to 11,400 km² at the
23
24 147 downstream limit.
25

26
27 148 The valley bottom presents an average width of 1.5-2 km, and is bordered by steep slopes
28
29 149 composed of porphyry and limestones or by alluvial fans built by tributaries. Downstream from
30
31
32 150 the city of Merano, channel slopes are quite low (<0.2 %) and rather constant for about 200 km,
33
34 151 despite the river flows through relatively high mountains peaks. Currently, this segment of the
35
36 152 Adige River features a straight to sinuous pattern and an average channel width of 58-82 m. As
37
38
39 153 retrieved from the Corine Land Cover database produced for 2012, the portion of the catchment
40
41 154 drained by the study segment is composed of 84% by forests and semi-natural areas (47%
42
43 155 forests; 18% shrubs and/or herbaceous vegetation associations; 19% open space with little or no
44
45
46 156 vegetation), 14% by agricultural areas and 2% by artificial surfaces. Along the study segment,
47
48 157 several important (up to 4,164 km² in drainage area) tributaries flow into the Adige River,
49
50
51 158 developing small to large alluvial fans. The terminal reaches of these tributaries across their
52
53 159 alluvial fans were also investigated in the present analysis (Figure 1). Total analyzed channel
54
55
56
57
58
59
60

1
2
3 160 length is about 29.2 km. Similarly to the Adige River, also the final reaches of the main
4
5 161 tributaries were interested by channelization during the 19th century.
6
7

8 162

9
10 163

11 12 13 164 **Methods**

14 15 165 *GIS-based morphological characterization of the river network*

16
17 166 The study was based on the analysis of 7 sets of historical maps dating between 1803 and 1927
18
19
20 167 (Table 1 and Figure 2). All sets cover the entire valley bottom in the segment from Merano to
21
22 168 Calliano. Historical maps come from several archives (Table 1), and were digitized using flatbed
23
24 169 cold-light scanner in multi-resolution format (bit depth RGB 24 bits, TIFF master files 600 dpi).
25
26
27 170 Afterwards, each map sheet was rectified in a GIS environment using the historical cadastral
28
29 171 map of 1856-1861 as reference map, as this was provided already in UTM-ETRS89 coordinates
30
31
32 172 by the Autonomous Province of Bozen/Bolzano and the Autonomous Province of Trento. A total
33
34 173 of 212 map sheets were georeferenced using from 10 to 20 Ground Control Points (GCPs),
35
36 174 mostly located in the proximity of the channel and by means of the application of a second-order
37
38 175 polynomial transformation. Root mean square position errors (RMSE) of residuals were in the
39
40 176 order of 1–27 m, with higher errors associated with the older maps.
41
42

43 177 The positional accuracy could appear important for such fine scale maps (from 3 to 10 times the
44
45 178 graphic error). Nevertheless, it should be underlined that this kind of maps presents additional
46
47 179 inaccuracies principally due to the material degradation of the paper as well as to their
48
49 180 digitization phase. Paper degradation – the more relevant issue – is typical of maps being over
50
51 181 200 years-old and is caused by two types of deformation: i) shrinkage of the original map due to
52
53 182 paper dehydration, and ii) stretching of the original map due to several subsequent reproductions
54
55
56
57
58
59
60

1
2
3 183 by heliography. The reference Habsburg Cadastre map (scale 1:2.880, corresponding to a graphic
4
5 184 error of 0.576 m) was checked measuring the distance between 2 points inside the range of 1 km,
6
7
8 185 both graphically on the map and by surveying on the terrain. A mean positional error of 6-8 m
9
10 186 per km was observed (Mastrorunzio and Dai Prà 2016a; 2016b).

11
12 187
13
14
15 188 The geomorphological analysis of the Adige River was subdivided into two steps: i) GIS-based
16
17 189 morphological characterization of the Adige River before channelization, (see Table 1); ii)
18
19
20 190 characterization of its evolution during the channelization works (until 1927).

21
22 191 The very large scale (1:3.456) map surveyed in 1803-1805 by the Austrian empire (“Nowack-
23
24 192 Plan”) – the most accurate of our database – was taken as a reference for channel segmentation.

25
26
27 193 The study river segment (115 km long) was divided into 42 homogeneous reaches (ranging in
28
29 194 length from 1 to 5 km), following the approach described by Rinaldi et al. (2013, 2015a), which
30
31
32 195 takes into account the occurrence of discontinuities as confluences with relevant tributaries,
33
34 196 changes in lateral confinement, in valley orientation, in valley slope and in channel width and
35
36 197 planform pattern. Channel pattern classification was also based on Rinaldi et al. (2013, 2015b),
37
38
39 198 whereby the following channel types were included: braided (B), anabranching (A), wandering
40
41 199 (W), sinuous with alternate bars (SAB), sinuous (S), meandering (M) and straight (St). Six
42
43 200 macro-reaches were later defined for the analysis of the evolution of the channel during the
44
45 201 channelization works, based on channel morphologies, valley orientations, confluences and
46
47
48 202 similarity with neighboring reaches. They range in length from 10 to 24 km.

49
50 203 The 7 sets of maps were digitized recognizing the occurrence of active channels, bars, islands,
51
52 204 and artificial structures in contact with banks. The quality and accuracy of the maps allowed the
53
54
55 205 recognition of bare alluvial sediments (classified as bars) and vegetated fluvial deposits included

1
2
3 206 in the active channel area (classified as islands). Two geodatabases related to the pre- and
4
5 207 during-channelization conditions, respectively, were derived. The first aimed at a detailed
6
7
8 208 analysis of the morphological patterns as mapped in 1803-1805. Twelve parameters were used to
9
10 209 characterize the morphology of each reach as defined in Table 2. The second database was based
11
12 210 on the six macro-reaches, and focused on channel evolution from 1803-1805 to 1915-1927, i.e.
13
14 211 on the effects of the channelization works, before other major anthropic alterations took place
15
16 212 (e.g. hydropower dams). A subset of 6 parameters was considered in this case, namely: average
17
18 213 channel width (W), bar ratio (B), island ratio (I), sinuosity index (SI), braiding index (BI),
19
20 214 anastomosing index (AI), (see also Table 2). In addition, the proportion of channel affected by
21
22 215 training structures as levees and ripraps, either on one or two banks, was evaluated as the ratio
23
24 216 between the length of the training works in direct contact with channel banks and the total bank
25
26 217 length measured along both banks (Bwk).

27
28
29 218 The potential influence of tributaries on the observed changes was investigated reconstructing
30
31 219 the morphological dynamics of the main tributaries (Passirio/Passer, Valsura/Falschauer, Rio di
32
33 220 Nova/Naifbach, Talvera/Talfer, Isarco/Eisack, Noce, Avisio, Fersina, see Figure 1). Note that
34
35 221 both Italian and German names are provided here only for the rivers lying in the Autonomous
36
37 222 Province of Bolzano. Their terminal segments (23 reaches in total) flowing across their alluvial
38
39 223 fans before joining the Adige were characterized through the following parameters: channel
40
41 224 width excluding islands (W), total channel width including island (Wt), bar ratio (B), island ratio
42
43 225 (I), basin area (BA) and bank length affected by work (Bwk).

44
45
46 226

47
48
49 227 *Analysis of morphological characteristics and evolution*
50
51
52

1
2
3 228 The geodatabases described above were processed through univariate and multivariate statistical
4
5
6 229 analysis, as well as in terms of evolutionary trajectories. The univariate analysis was used to
7
8 230 evaluate the variability of parameters in space and time. Multivariate analysis consisted of a
9
10 231 Principal Component Analysis (PCA) and a hierarchical clustering analysis (HCA) and were
11
12 232 applied to the databases characterizing the Adige River before the channelization works. The
13
14
15 233 PCA was used to reduce the dimensionality of the initial datasets, through linear combinations of
16
17 234 the original variables. The first four components resulting from the PCA were used to perform a
18
19
20 235 hierarchical clustering analysis aimed at grouping reaches with homogeneous properties. A
21
22 236 Principal Component Analysis (PCA) was also used to investigate the relation between the initial
23
24 237 six variables analyzed for the tributaries in 1803-1805.

25
26
27 238 In order to investigate the relationship between observed channel changes and controlling
28
29 239 factors, the available information on natural as well as on anthropic pressures in the Adige River
30
31
32 240 basin (from the reach to the catchment scale) was collected. River discharge and sediment
33
34 241 transport data were not available for the analyzed period, therefore, the potential influence of
35
36 242 climatic variations on channel evolution was inferred from i) local historical flood events
37
38 243 (available from the Autonomous Province. of Bolzano); ii) recent studies on past climate trends
39
40 244 in the Alps (Brunetti et al., 2000, 2001, 2006); and iii) glaciological evidences (Fischer et al.,
41
42 245 2015), similarly to what done by Marchese et al. (2017).

43
44
45 246 Bank protection and land cover changes were considered as the main anthropic factors. Despite
46
47 247 few retention check-dams were already built in the late 19th century in some of the Adige's
48
49 248 tributaries, torrent control works were widely constructed only after WWI and more intensively
50
51 249 after WWII (see also Comiti, 2012 and Campana et al., 2014), and the oldest hydropower
52
53 250 structure in the catchment dates to 1926. Finally, forest cover changes at the catchment scale
54
55
56
57
58
59
60

1
2
3 251 were analyzed putting together the existing literature on specific sub-catchments of the Adige
4
5 252 basin (Tasser et al., 2007; Marchese et al., 2017) with unpublished results deriving from the
6
7
8 253 comparison of two land use maps (1855 and 1970) covering the entire Autonomous Province of
9
10 254 Bolzano (65% of the considered Adige basin area). Forest areas in the former map (the Cadastral
11
12 255 map above mentioned) were digitized based on an automatic and supervised detection process
13
14
15 256 available within ArcGIS (Image Analysis tool).
16
17
18 257

19
20 258 *Application of analytical morphodynamic models and channel pattern predictors*
21

22 259 A morphodynamic analytical theory for river bars and two rational channel pattern predictors
23
24 260 were applied to the 42 reaches as well as to the six macro-reaches described earlier. In particular,
25
26
27 261 we compared results from the theory of free bars proposed by Colombini et al. (1987), the
28
29 262 physics-based river bar and channel pattern predictor proposed by Crosato and Mosselman
30
31 263 (2009), and the rational channel pattern predictor proposed by Eaton et al. (2010). For the sake of
32
33
34 264 readability in the following we will refer to these three approaches, respectively as “free-bar
35
36 265 predictor”, “hybrid-bar predictor” (e.g. Durò et al., 2016) and “channel pattern predictor”. The
37
38
39 266 free and the hybrid bar predictors are based on the linear solution of the complete 2D (depth-
40
41 267 averaged) morphodynamic equations for longitudinal and transverse momentum together with
42
43
44 268 the continuity equations for water and sediments.

45
46 269 The free-bar theory (Colombini et al., 1987) predicts free bars to occur in idealized, infinitely
47
48 270 long channels because of an intrinsic instability of the system resulting from the interaction
49
50 271 between the water flow and the mobile channel bed. Only in enough wide and shallow channels,
51
52
53 272 such instability arises, leading to free-bar formation. Despite being strictly valid for indefinitely
54
55 273 long and straight channels, the free-bar predictor can be applied to predict the tendency of an
56
57
58
59
60

274 alluvial river to form alternate bars. The key parameter controlling such instability is the width to
 275 depth ratio (β) of the channel at bar-forming conditions. When β exceeds a critical value β_c bars
 276 will develop, while for $\beta < \beta_c$ bars are damped and the flat bed is stable. The threshold depends
 277 on the reach-averaged values of the Shields parameter, a measure of sediment mobility, and of
 278 the ratio between a representative reach-averaged sediment size and flow depth. For sake of
 279 clarity, it is important to remark that in some theoretical papers the same symbol β is used to
 280 denote the half channel width to depth ratio, instead of the width to depth ratio as in the present
 281 paper.

282 The hybrid-bar predictor allows the estimation of the most likely number of bars that will form in
 283 a cross-section, considering a straight channel reach with a finite length. The number of bars in a
 284 cross-section is represented through a “bar mode”, denoted with m in the following. The basic
 285 unit $m = 1$, represents the case of alternate bars, while larger values of m correspond to a larger
 286 number of bars in each cross-section, increasing from central bars ($m = 2$) to multiple bars ($m >$
 287 3). The hybrid bar predictor (Crosato and Mosselman, 2009) returns a numerical value of the bar
 288 mode m through the equation (1):

$$m = \left[0.17g \frac{(b-3) W^3 S_c}{\sqrt{\Delta} D_{50} C Q} \right]^{1/2}, \quad (1)$$

290 where W is the channel width, g is gravitational acceleration, C is the dimensional Chezy
 291 coefficient for hydraulic resistance, Q is a bar-forming value of flow discharge, D_{50} is the
 292 median sediment size, Δ is the submerged relative density, S_c represents the river slope and b
 293 quantifies the degree of nonlinearity of the bedload transport equation, expressed as a relation
 294 between bedload rate and flow velocity. For the present analysis we used $b = 10$, as suggested for
 295 gravel bed rivers (Crosato and Mosselman, 2009).

1
2
3 296 The rational channel pattern predictor proposed by Eaton et al (2010) is derived from the
4
5
6 297 combination of principles of hydraulic geometry and an extremal hypothesis of maximum
7
8 298 sediment transport efficiency (Millar, 2005). It first adopts the value of $\beta = 50$ previously
9
10
11 299 proposed as threshold value discriminating between single- and multi-thread channels. As a
12
13 300 result the method yields a critical value of the channel slope S_N for a river pattern characterized
14
15 301 by N separate parallel channels, indicating in $N = 4$, the threshold between stable
16
17
18 302 (meandering/anabranching) and unstable (braided) multiple-thread channels.

19
20 303 The expression for such discriminant function reads:

21
22 304
$$S_N = 0.40N^{0.43}\mu'^{1.41}Q^{*-0.43}, (2)$$

23
24
25 305 where μ' indicates the dimensionless bank strength as ratio between the critical shear stress for
26
27 306 the bank toe and the critical shear stress for the channel bed, and Q^* is a dimensionless discharge,
28
29 307 defined as:

30
31
32 308
$$Q^* = \frac{Q}{D_{50}^2\sqrt{\Delta g D_{50}}}, (3)$$

33
34
35 309
36
37 310 The study of Eaton et al. (2010) also proposes a theoretical relation to predict the number of
38
39 311 channel anabranches N (their equation 8), which can then be explicitly expressed in terms of the
40
41 312 flow discharge Q , the sediment size D_{50} and the channel slope S :

42
43
44 313
$$N = 2.09 Q S^{2.32} D_{50}^{-2.5} \mu'^{-3.28} \quad (4),$$

45
46
47 314 a relation which, however, has not been explicitly tested by the authors. Rigorous estimation of
48
49 315 the parameter μ' would require targeted field measurements or existing data to quantify the
50
51 316 critical shear stress at the bank toe and at the channel bed, which are not available, particularly in
52
53 317 relation to the historical conditions. As also implicit in the work of Eaton et al. (2010), the
54
55 318 parameter μ' can be used as a calibration parameter. We therefore explored the effect of
56
57
58
59
60

1
2
3 319 changing μ' in the meaningful range suggested by Eaton et al (2010), i.e. from 1 (no significant
4
5
6 320 vegetation effect on bank cohesion) to 5 (very high bank reinforcement by vegetation). The
7
8 321 pattern of every reach has been computed through equation (2) for several values of μ' in the
9
10 322 range 1 to 5, and the percentage of correctly predicted patterns has been assessed. A unique
11
12 323 representative value of $\mu' = 1.5$ for the whole segment was chosen as it maximizes the number
13
14 324 of correctly predicted reach morphologies.

15
16
17 325 To compare the outputs of the hybrid bar predictor (most probable bar mode m) and of the
18
19 326 channel pattern predictor (type of channel pattern) we adopted the threshold values for the bar
20
21 327 mode m proposed by Crosato and Mosselman (2009). The lower threshold, $m = 1.5$, indicates a
22
23 328 transition zone between single-thread and transitional channel planforms. The upper threshold,
24
25 329 $m = 2.5$, indicates a transition zone between transitional and braided patterns. The hybrid bar
26
27 330 predictor does not discriminate between stable (i.e., anabranching) and unstable (i.e., braided)
28
29 331 channel patterns, a distinction which is made by the channel pattern predictor.

30
31
32 332 Both free and hybrid-bar predictors and the channel pattern predictor require similar, reach-
33
34 333 averaged, input parameters: formative discharge, channel slope, and the sediment size
35
36 334 representative for the channel bed surface, D_{50} (Table 3). In addition, the bar predictors require
37
38 335 an input reach-averaged channel width, while the channel pattern predictor needs an estimate of
39
40 336 the relative bank strength. It is here worth to mention that both bar theories and pattern predictor
41
42 337 refer to channels which are under equilibrium with respect to the hydrological regime and
43
44 338 sediment supply. Presently, the Adige is strongly armored and its surface median grain size
45
46 339 cannot be assumed representative for the 19th century channel bed material. Therefore, we used
47
48 340 the sub-surface grain size distribution to estimate the input sediment size for the bar and channel
49
50 341 pattern predictors, assuming that it was less impacted by human interventions. As no historical
51
52
53
54
55
56
57
58
59
60

1
2
3 342 information on the grain size is available, the median sediment size D_{50} was estimated from
4
5 343 samples collected from six different locations well distributed along the 115 km study reach, thus
6
7
8 344 yielding a representative grain size value for each macro-reach. In the light of the intrinsic
9
10 345 uncertainties in determining an input grain size value, we assessed the sensitivity of the outcome
11
12 346 of the bar and pattern predictors to the sediment size by increasing D_{50} up to 50%. Formative
13
14 347 discharge values were estimated from historical daily discharge records available at the gauging
15
16 348 stations of Ponte Adige, Bronzolo and Trento S. Lorenzo (see Figure 1). These three stations
17
18 349 were selected because of the long period covered by the measurements, approximately from
19
20 350 1920 to 2010, and because of their location, which isolates the discharge contribution of the main
21
22 351 lateral tributaries. To cope with the intrinsic uncertainty associated with the estimate of a
23
24 352 constant value of a “formative discharge”, the discharge values with recurrence interval greater
25
26 353 than 2, 5, and 10 years (Q_2 , Q_5 , Q_{10}) were computed for each station by fitting the streamflow
27
28 354 records with a Gumbel distribution. Because of the absence of relevant lateral tributaries within
29
30 355 the macro-reaches and because of the relative position of the gauging stations, data from Ponte
31
32 356 Adige (located in M2) are representative of macro-reaches M2 and most of M1, Bronzolo
33
34 357 (located in M3) of M3 and M4, Trento S. Lorenzo (located in M6) of M6 and also M5, for which
35
36 358 the overestimation associated with the confluence of the Avisio River (between M5 and M6)
37
38 359 does not have significant effects on the predictors outcomes. To roughly address the lack of
39
40 360 consistent hydrological data for the 19th century, we used the 20th century records as a reference,
41
42 361 and we hypothesized a possible two-fold increase of the flood frequency during the LIA, on the
43
44 362 basis of the available historical flood events database mentioned above. This means, for instance,
45
46 363 that the value of Q_{10} during the 19th century was computed as the value of Q_{20} obtained from the
47
48 364 present record.
49
50
51
52
53
54
55
56
57
58
59
60

1
2
3 365 This choice stems from available datasets from the Bolzano Province, which highlight higher
4
5 366 frequencies of floods, in the period between the 1860s and the end of the 1880s, especially
6
7 367 during the 1880s (Figure 9c and 1882, 1883, 1885, 1888, 1889, 1890, Turri and Ruffo, 2005).
8
9 368 The data in Figure 9c consider both the floods occurred in the overall Adige basin, and the flood
10
11 369 events only occurred in the reaches from 1 to 25 (within the Bolzano Province). Though such
12
13 370 observations clearly differ in accuracy and consistency from the present flow records, they
14
15 371 represent the only available source of information to formulate reasonable hypotheses for the
16
17 372 estimation of input streamflow values for the application of the bar and pattern predictors.
18
19 373 The increasing floods coupled to the increasing population density led to the first phase of
20
21 374 massive embankment and rectification along the Adige as in other larger unconfined rivers
22
23 375 (Hohensinner et al., 2004; Zawiejska and Wyzga, 2010; Hohensinner et al., 2013a; Hohensinner
24
25 376 et al., 2013b).
26
27
28
29
30
31
32
33

34 378 **Results**

35
36 379

37 380 *Channel morphology before channelization*

38
39 381 In 1803-1805, the Adige River in the segment under investigation was characterized by a
40
41 382 prevalence of single-thread patterns (73% in terms of total length), represented by sinuous
42
43 383 (34%), sinuous with alternate bars (24%) and meandering (15%) channel morphologies. Multi-
44
45 384 channel patterns represented 27% of the length, with braided dominating over anabranching (9%
46
47 385 vs 5%). The transitional wandering morphology characterized 13% of the channel length.
48
49 386 Descriptive univariate and multivariate analysis were used to characterized the Adige, from a
50
51 387 geomorphological point of view.
52
53
54
55
56
57
58
59
60

1
2
3 388 As expected, univariate descriptive analysis shows that the analyzed variables present specific
4
5 389 ranges for each channel morphology (Figure 3). Among these, channel width decreases from the
6
7
8 390 braided and anabranching pattern to the sinuous and meandering (Figure 3a). Channel width of
9
10 391 multi-thread reaches is wider also when including the vegetated islands (Figure 3b) especially for
11
12 392 the anabranching reaches. The islands ratio is obviously higher in the anabranching reaches,
13
14 393 followed by braided reaches (Figure 3c) and then it becomes very small in other patterns. More
15
16 394 interesting is to note how the bar ratio features an average value exceeding 0.3 in the multi-
17
18 395 thread reaches as well as in the sinuous with alternated bars reaches, and below 0.3 in the
19
20 396 sinuous and meandering reaches (Figure 3d). On average, the width of the alluvial plain is about
21
22 397 1470 m, and the largest values occur in correspondence to sinuous with alternate bars and
23
24 398 anabranching morphologies (Figure 3e). Wandering reaches are characterized by the narrowest
25
26 399 alluvial plain. However, when normalized by channel width (i.e. confinement index), sinuous
27
28 400 with alternate bars and sinuous reaches are the least confined, and braided and wandering
29
30 401 patterns feature the highest confinement (i.e. the lowest confinement index, figure 3f). Valley
31
32 402 and channel slopes (S_v , S_c) are higher in the multi-thread morphologies and decrease for
33
34 403 transitional and single-thread patterns. In particular, valley slope is on average 0.31 % for the
35
36 404 braided, 0.17 % and 0.13 % for the wandering and anabranching, respectively, and it is as low as
37
38 405 0.08 % in the meandering and sinuous reaches (Figure 3g). Univariate distribution of the distance
39
40 406 from the main upstream tributary (Figure 3h) indicates that braided and wandering patterns are
41
42 407 more likely to be located few hundreds of meters downstream of the main confluences, whereas
43
44 408 this distance exceeds 1000 m for single-thread reaches.

45
46
47
48
49
50
51
52
53 409 A multivariate analysis was carried out using the 1803-1805 dataset on channel morphology,
54
55 410 using the 12 variables reported in Table 2. The PCA led to 4 principal components, representing
56
57
58
59
60

1
2
3 411 85% of the total variance, with the first component accounting for 46%. This mainly presents a
4
5
6 412 negative correlation with channel width, also when including islands (W and W_{tot}), with bar ratio
7
8 413 (B) and with braiding and anastomosing indices (BI , AI) (Figure 4a). As expected, such
9
10 414 dominant component summarizes the quantitative channel characteristics that are used in the
11
12 415 definition of the channel pattern. The second component represents 17% of the total variance and
13
14 416 seems to characterize the width of the river corridor. In particular, it shows a negative correlation
15
16 417 with the alluvial plain width (AP) and the confinement index (CI) (Figure 4a). The third
17
18 418 component represents 12% of total variance, and results to be negatively correlated with valley
19
20 419 (S_v) and channel slopes (S_c), thus possibly reflecting the “potential energy” condition of the
21
22 420 reaches. Finally, the fourth component, accounting for 9% of the total variance, is negatively
23
24 421 correlated with the sinuosity index (S) and positively with the distance from the first main
25
26 422 tributary upstream (T), and thus it could be associated with the role of lateral forcing in terms of
27
28 423 sediment supply. Figure 4a shows also the correlation of each reach with the first and second
29
30 424 components (axes), with a clear difference between single-thread reaches, on the right side of the
31
32 425 plot, and multi-thread morphologies on the left side of the plot.
33
34
35
36
37
38
39
40

41 427 A hierarchical clustering analysis was performed on all the Adige reaches using the first 4
42
43 428 components resulting from the PCA analysis described above. The result of this clustering are
44
45 429 four groups of reaches sharing high similarities in terms of overall morphological characteristics
46
47 430 as well as external factors (Figure 4b and Table 4). Group 1 (16 reaches) comprises reaches with
48
49 431 single-thread morphologies, especially sinuous and sinuous with alternated bars (Table 4). Group
50
51 432 2 (13 reaches) is similar to the previous one as it is characterized by single-thread morphologies,
52
53 433 but in this case meandering and sinuous patterns prevail. The most significant parameter for this
54
55
56
57
58
59
60

1
2
3 434 group is the high sinuosity index (Table 4). Reaches belonging to groups 1 and 2 are located at
4
5
6 435 considerable distance from the main upstream tributary (Table 4). Group 3 (only 2 reaches)
7
8 436 includes two multi-thread reaches with anabranching and braided morphologies, respectively.
9
10 437 They are characterized by high presence of bars and islands. Group 4 (11 reaches) includes
11
12 438 multi-thread reaches characterized by wandering and braided morphologies. These reaches are
13
14 439 located immediately downstream of the main tributaries.

15
16
17 440 The location of these four groups along the Adige suggests that they are not randomly
18
19
20 441 distributed. Indeed, these groups were the basis to combine the initial reaches into macro-
21
22 442 reaches, which overall show a longitudinal alternation between multi-thread and single-thread
23
24 443 reaches (Figures 4b and 4c). Division in macro-reaches is based on distribution of channel
25
26 444 morphologies from upstream to downstream and on similarity with neighboring reaches. More
27
28 445 specifically, macro-reaches M1, M3, M5 (Figures 4b and 4c) are composed by alternate multi-
29
30 446 thread and single-thread morphologies, but in general the multi-thread reaches prevail in length.
31
32 447 Macro-reaches M2, M4 and M6 are exclusively composed of reaches characterized by single-
33
34 448 thread morphologies (Figures 4b and 4c).

35
36
37 449 Figure 5 visually compares the outcomes of the hybrid-bar and channel pattern predictors with
38
39 450 observations of the channel pattern before channelization, and the outcomes of the hybrid-bar
40
41 451 predictor with observations after channelization. The observed and predicted morphologies are
42
43 452 denoted with different intensities of blue in the lower part of the figure, with increasing intensity
44
45 453 of blue corresponding to increasing morphological complexity. Overall, predictions of pre-
46
47 454 channelization channel morphology compare rather well with observations. The comparison has
48
49 455 been considered successful when an observed multi-thread (i.e., braided, anabranching) or a
50
51 456 single-thread (i.e., straight, sinuous, meandering) pattern is correctly predicted. Specifically, the
52
53
54
55
56
57
58
59
60

1
2
3 457 dominant morphology for every macro-reach (M1 to M6) is correctly predicted by both
4
5
6 458 predictors in 5 out of 6 cases, and for a total length of 88% of the analyzed river segment. The
7
8 459 two predictors are less performing when the pattern of every single reach is compared, with the
9
10 460 channel pattern predictor of Eaton et al. (2010) correctly reproducing a slightly higher proportion
11
12 461 ($55.5\% \pm 3.5\%$, considering the uncertainty of discharge and grain size) of patterns in
13
14 462 comparison with the hybrid bar predictor of Crosato and Mosselman ($48\% \pm 5\%$).
15
16
17 463 Despite these local discrepancies at the individual reach scale, both predictors suggest the
18
19 464 tendency of the Adige River to develop multi-thread morphologies immediately downstream of
20
21 465 the confluences with major lateral tributaries, whose locations are denoted with vertical black
22
23 466 arrows in Figure 5. Also the observed tendency to a single-thread pattern further downstream of
24
25 467 the major confluences is broadly predicted. Such tendency is consistent with observations from
26
27 468 the 1803-1805 map, already shown in Figures 4 and 5, downstream of the confluences with the
28
29 469 Valsura, Isarco and Noce rivers, and with the exception of the observed patterns immediately
30
31 470 downstream of the confluence with the Fersina River that does not determine relevant changes in
32
33 471 Adige channel morphology.
34
35
36
37
38
39
40

41 473 *Channel evolution during the 19th century*

42
43 474 The analysis of channel evolution during the 19th until the early 20th century is presented
44
45 475 referring to the 6 macro-reaches defined in the previous section (see Figure 4). In order to
46
47 476 analyze the temporal changes, the evolutionary trajectories relative to the morphological
48
49 477 parameters were reconstructed (Figure 6). The parameters describing the channel morphology
50
51 478 and the abundance of bars and islands show dramatic changes between 1803 and 1917. However,
52
53
54
55
56
57
58
59
60

1
2
3 479 some differences in their evolutionary trajectories are separately highlighted for macro-reaches
4
5
6 480 characterized by multi-thread and single- thread patterns in 1803.

7
8 481 Channel width in the macro-reaches characterized by an initial multi-thread pattern (Figure 6a)
9
10 482 shows fluctuations until 1847. Between 1847 and 1855 the channelization took place in most of
11
12 483 these reaches, and thus narrowing started, progressing further until 1905, when channel widths
13
14 484 were reduced by - 40% to - 70% of the initial value. The narrowing trend was concurrent to
15
16 485 important and progressive pattern changes (Figure 6b). The multi-thread morphologies were
17
18 486 gradually substituted by sinuous and straight morphologies. By 1905, the multi-thread
19
20 487 morphologies were only 6%, while they were 67% in 1803.

21
22 488 Remarkably, channel widths in the single-thread macro-reaches were quite stable until 1870
23
24 489 (Figure 6e). Afterwards, the narrowing started reaching - 40% by 1905, and it strongly slowed
25
26 490 down between 1905 and 1917. In these macro-reaches, meandering, sinuous and sinuous with
27
28 491 alternate bars morphologies were largely replaced by straight, artificial channels (Figure 6f).

29
30 492 Modifications in channel width also affected bar and island occurrence and the related braiding,
31
32 493 anabranching, and sinuosity indices. Bar and island ratios decreased at a faster pace between
33
34 494 1816 and 1855. Indeed, islands almost completely disappeared by 1855, earlier compared to the
35
36 495 disappearance of bars (Figures 6c and 6g). Multi-thread reaches maintained a relevant bar ratio
37
38 496 up to 1905 (Figure 6c), whereas in the single-thread macro-reaches (Figure 6g) bar ratio was
39
40 497 highly reduced already in 1855. Especially after 1847, bars in the single-thread reaches
41
42 498 disappeared also without any significant decrease in channel width (Figure 6e and 7g).

43
44 499 The post-channelization channel morphology is correctly predicted for 88% of the 42 individual
45
46 500 reaches by the hybrid-bar predictor of Crosato and Mosselman (2009), such percentage being
47
48 501 almost identical in terms of length of predicted morphology of macro-reaches.

1
2
3 502 Overall, the analysis showed a strong simplification of the channel system between the beginning
4
5 503 of the 19th century and the beginning of the 20th century.
6
7

8 504
9

10 505 *Morphology of the main tributaries and their evolution*
11

12 506 The terminal reaches of the main tributaries of the Adige River were investigated considering
13
14 507 their morphology in 1803-1805 and the channel evolution over the analyzed period.
15
16

17 508 A PCA analysis was performed, obtaining a reduction of the initial six variables (W , W_{tot} , BA ,
18
19 B , I , Bwk) to 2 principal components representing 80% of total variance. The first component
20 509 (B , I , Bwk) to 2 principal components representing 80% of total variance. The first component
21
22 510 (44% of total variance) shows a negative correlation with channel width, also including islands
23
24 511 (W and W_{tot}), and the island ratio (I), similarly to what we obtained for the first component of the
25
26 512 Adige River in 1803-1805. The second component represents 36% of total variance, has a
27
28 513 negative correlation with the bar ratio (B) and a positive correlation with the basin area (BA).
29
30

31 514 The evolutionary trajectories analyzed in terms of average channel width, bar ratio and islands
32
33 515 ratio for all these tributaries show an overall channel narrowing and simplification of channel
34
35 516 morphology between 1803 and 1917 (Figure 7). Channel widths decreased mostly between 1847
36
37 517 and 1855 when, compared to 1803, they reached values of – 57% on average, and maximum of –
38
39 518 85% (Figure 7a). Between 1803 and 1855 bar cover declined (Figure 7b) from 70% of the total
40
41 519 area to 30% on average. The decrease in bar ratio slowed down between 1855 and 1870 (Figure
42
43 520 7b) and then again accelerated between 1905 and 1917. Island ratio started to decrease already
44
45 521 from 1803 (when it was equal to 8% on average considering all the tributaries), as in 1816 it
46
47 522 reached values of about 1%. Few exceptions are present, such as the anabranching reaches
48
49 523 belonging to terminal reaches of the Valsura and Avisio rivers. Island ratios were stable with
50
51 524 high values (30%) until 1847, as in the case of the the Valsura, and for the Avisio until 1905.
52
53
54
55
56
57
58
59
60

1
2
3 525 Therefore, channel morphology in these terminal reaches underwent severe modifications
4
5 526 (Figure 7d). Between 1847 and 1855, anabranching channels disappeared, braiding markedly
6
7
8 527 decreased, and straight morphologies significantly increased. Since 1855, straight channels were
9
10
11 528 the prevalent patterns. Embankments in studied tributaries increased especially between 1803
12
13 529 and 1870, whereas afterwards they remained rather stable (Figure 7c).
14

15 530

17 531 *Application of free-bar predictor*

19
20 532 Figure 8 shows the results of the application of the free-bar predictor to the six macro-reaches
21
22 533 before and after channelization, in terms of the difference $\beta - \beta_c$ between the width to depth
23
24 534 ratio β and its critical value for free bars formation β_c . Positive values of this parameter imply
25
26
27 535 bed instability, thus bar formation, whereas negative values are associated with flat bed. As
28
29 536 specified in the method section, we considered Q_2 , Q_5 , Q_{10} to characterize the present
30
31
32 537 hydrological regime, and Q_5 , Q_{10} , and Q_{20} to take into account an approximate twofold increase
33
34 538 of flood frequency during the LIA. In Figure 8, blue filled circles refer to the pre channelization
35
36 539 configuration with the present hydrology, the red asterisks show the effect of increasing the
37
38
39 540 discharge to the hypothesized LIA values, and finally the black open circles correspond to the
40
41 541 post channelization conditions. Higher points of each set refer to the lower discharge value in the
42
43
44 542 examined range, as in this condition the width to depth ratio β is higher and the critical threshold
45
46 543 β_c is lower. Outcomes of the model clearly show a tendency to form bars with any combination
47
48 544 of parameters in the pre channelization configuration (positive values), whereas present
49
50
51 545 conditions are likely to be slightly unstable for the three most upstream macro reaches and
52
53 546 clearly stable (no bar formation) for the three more downstream. Strictly speaking, only for M6
54
55 547 (pre-channelization) and M3 (post-channelization) the choice of formative discharge may be
56
57
58
59
60

1
2
3 548 relevant to predict whether the width to depth ratio β crosses the bar stability threshold β_c .
4
5
6 549 However, it has to be remarked that such threshold must not be intended as a sharp border, also
7
8 550 in relation to the uncertainties in the input parameters and in the assumptions of the theory. The
9
10 551 analysis of the effect of modifying the sediment size proved no major impact on the free-bar
11
12 552 predictor, with small variations of the $\beta - \beta_c$ parameter (up to 10%), and larger overall
13
14 553 variations of each of the parameters β and β_c (within 25%). Most importantly, the examined
15
16 554 variability in sediment size did not produce changes in the tendency of the macro reaches to form
17
18 555 free bars.
19
20
21
22 556 These results compare well with observations from historical maps. Bars were present along the
23
24 557 whole study reach before channelization (e.g. figure 3d), both in multi-thread (Figure 6c) and
25
26 558 single-thread macro reaches (Figure 6g). Moreover, macro-reaches M1, M3, M5 showed a higher
27
28 559 morphological complexity compared to macro-reaches M2, M4, M6, and are characterized by
29
30 560 higher values of the difference $\beta - \beta_c$, which theoretically corresponds to a higher
31
32 561 morphological complexity of the river pattern.
33
34
35
36 562 Figure 8 also shows the theoretical effect of channel narrowing associated with channelization,
37
38 563 when looking at the corresponding markers that refer to the discharge with the same return
39
40 564 interval. Indeed, artificial narrow width strongly reduced the tendency of the Adige River to
41
42 565 develop free bars (i.e., the difference $\beta - \beta_c$), especially for the braided and wandering sections,
43
44 566 which were subjected to the most intense reduction of their width. In the new configuration,
45
46 567 macro-reaches M4, M5 and M6, lie below the bar-forming threshold for all the analyzed
47
48 568 discharges, in agreement with the observation that bars are not observed anymore after
49
50 569 channelization (Figure 6c and 6g).
51
52
53
54
55
56 570

1
2
3 5714
5
6 572 **Discussion**7
8 5739
10 574 *Adige River before channelization: insights from historical analysis and theoretical approaches*11
12 575 The analysis of the Adige River morphology before channelization showed the presence of13
14 576 homogeneous macro-reaches, characterized by prevalence of single-thread or multi-thread15
16 577 patterns. At the very beginning of the 19th century, i.e. before major human disturbances, the17
18 578 Adige River already presented a prevalent single-thread planform morphology within its19
20 579 montane basin, in contrast to other large rivers of the Southern Alps characterized by steeper21
22 580 valley slopes (Surian et al., 2009b; Comiti et al., 2011; Ziliani and Surian, 2012; Moretto et al.,23
24 581 2014). Sinuous and sinuous with alternate bars were the dominant patterns in the upper and25
26 582 middle part of the studied segment. The river channel was quite rich in bars, suggesting a27
28 583 relatively high supply from the catchment. Meandering was prevalent in the most downstream29
30 584 reaches, where the large point bars at meander bends may also indicate a regular bedload31
32 585 transport.33
34 586 Indeed, at the beginning of the 19th century, sediment supply entering the main Alpine rivers35
36 587 from their headwaters was probably very high – i.e. higher than in both preceding and37
38 588 subsequent centuries – due to the effects of the Little Ice Age, to a lower forest cover, as well as39
40 589 to the very limited presence of controlling works (Comiti, 2012). High sediment dynamics at the41
42 590 basin scale is evidenced by the abundance of bars in the terminal reaches of the main tributaries43
44 591 of the Adige River, where most reaches presented complex planforms (wandering or braided45
46 592 patterns), even when controlled by bank protection. Such morphologies testify the large sediment47
48 593 amount produced and transported to the outlet of these sub-catchments during the 19th century. A

1
2
3 594 remarkable feature of the Adige planform before channelization was the presence of
4
5 595 anabranching reaches, characterized by multiple, relatively stable secondary channels with large
6
7
8 596 forested islands. At that time, this pattern was quite common in mild-sloping (0.1–0.3%), wide
9
10
11 597 valleys of the Alps (Comiti, 2012; Campana et al., 2014) as well as in other large European
12
13 598 rivers, such as the Danube (Hohensinner et al., 2013a and 2013b).

14
15 599 Before channelization, tributaries had a major effect on the Adige River morphology, imparting
16
17 600 multi-thread patterns (braided and anabranching) immediately after their confluences (Figures 4
18
19
20 601 and 10). This was likely due to the high amount of coarse sediments carried by the (much
21
22 602 steeper) tributaries, which induced transient sediment deposition in the Adige River, promoting
23
24 603 the formation of numerous large gravel bars and islands. Downstream of these multi-thread
25
26
27 604 reaches, transitional reaches 1-2 km long would generally follow, developing then into a single-
28
29 605 thread pattern. Multi-thread reaches were in most cases characterized by a dense cover of
30
31 606 riparian vegetation.

32
33
34 607 Both the hybrid bar and the channel pattern predictors were able to consistently estimate the
35
36 608 channel pattern before the major embankment works, at the scale of the macro-reaches (Figure
37
38
39 609 8). Both predictors use the width to depth ratio as the controlling parameter, though with a
40
41 610 fundamental difference: the channel pattern predictor computes an equilibrium channel width,
42
43 611 which is instead given as input to the hybrid pattern predictor as resulting from the analysis of
44
45
46 612 the historical maps. At the macro-reach scale, the equilibrium width predicted by Eaton et al.
47
48 613 (2010) does not differ much from the one resulting from the historical analysis, which suggests
49
50 614 the Adige River may have had a bankfull width that was approximately in equilibrium with the
51
52
53 615 hypothesized discharge, slope and grain size.

1
2
3 616 Both predictors are based on a somehow similar assumption of dynamic equilibrium of the river
4
5
6 617 channel, which refers to the spatial scale of long enough river reaches characterized by nearly
7
8 618 homogeneous boundary conditions. Therefore, it seems reasonable that the predictive ability of
9
10
11 619 the predictors is higher at the macro-reach scale compared to the scale of the local reach, because
12
13 620 smaller differences among individual reaches are filtered and only the average properties are
14
15 621 retained at the macro-reach scale.

16
17 622 The sequence of different planform configurations, from braided/anabranching to sinuous with
18
19
20 623 alternate bars and finally to sinuous or meandering reaches (Figure 4), represents an interesting
21
22 624 example of the longitudinal shift from multithread to single-thread observed also in other river
23
24 625 systems (Church, 2002; Beechie et al., 2006; Beechie and Imaki, 2014). The cause for this shift
26
27 626 has been associated to decreasing channel slope and thus transport capacity, and/or increasing
28
29 627 sediment supply and grain size (Schumm, 1985; Rice and Church, 1998; Church, 2002; Benda et
30
31 628 al., 2003; 2004; David et al., 2016).

32
33
34 629 As to the Adige River, because sediment supply from tributaries is only implicitly incorporated
35
36 630 in the predictors within the input values of channel slope, discharge, coarse sediment size (and
37
38 631 channel width for the hybrid bar predictor), the comparison between prediction and observation
39
40 632 suggests that tributaries affect the downstream channel morphology mostly by delivering coarse
41
42 633 sediments to a much lower energy channel, thus determining local bed steepening.

43
44
45 634

46 47 48 635 *Evolutionary trajectory of the Adige River*

49
50
51 636 The performed analysis shows that the Adige River underwent notable channel changes between
52
53 637 the 19th and the beginning of the 20th century, which occurred through three distinct phases
54
55 638 (Figure 9). The macro-reaches initially presenting a multi-thread pattern show slightly different
56
57
58
59
60

1
2
3 639 evolutionary trajectories compared to those with a prevalent single-thread morphology (Figure
4
5 640 9). In particular, as expected, channel narrowing was on average significantly higher in the
6
7 641 multi-thread macro-reaches where it was up to -87%, compared to the single-thread macro-
8
9 642 reaches where it was up to -50%.

10
11
12 643 During the first phase, between 1803 and 1847, channels were quite stable, with a few multi-
13
14 644 thread reaches experiencing minor widening between 1803 and 1816 (Figure 9a). During this
15
16 645 first phase, the presence of bank protections increased from values not exceeding 10% in 1803 to
17
18 646 about 30% in 1847 (Figure 9a). Furthermore, channel widths and channel morphologies in
19
20 647 tributaries remained stable in this period (Figure 9b). On the other hand, a considerable reduction
21
22 648 seems to have occurred in the areal extension of bars, both in Adige River and its tributaries
23
24 649 (Figure 9a and 9b). Although bars shown in the maps are influenced by the variability of
25
26 650 discharge - that exposes or submerges part of river bed at different flows-, we are convinced that
27
28 651 reduction or even absence of bars is clearly evident and is explained as correlated with the low
29
30 652 width-to-depth ratio imposed to the channelized channel (see the section *Application of free-bar*
31
32 653 *predictor*).

33
34
35
36
37
38 654 The period between 1847 and 1905 corresponds to the second phase of adjustment, but some
39
40 655 differences in time and intensity of processes can be considered within this phase. Between 1847
41
42 656 and 1855, multi-thread and tributary reaches underwent a first important channel narrowing,
43
44 657 while the single-thread reaches remained stable (Figure 9). Anabranching reaches had
45
46 658 progressively turned into wandering and single-thread patterns, with a much lesser extent of bars
47
48 659 and islands. Overall, we think that most of the channel changes observed during this period
49
50 660 (1847-1855) in the Adige River and its tributaries can be associated to channelization works,
51
52 661 which already suffered a consistent increase (80% of stabilized banks in the tributaries and 40%

1
2
3 662 in the Adige River, in 1855; Figure 9a and 9b). Between 1855 and 1870, channel widths in the
4
5 663 single-thread reaches on average decreased, in the multi-thread on average was constant and in
6
7 664 terminal reaches of main tributaries slightly increased (Figure 9). In the Adige River some
8
9 665 increase of sinuous with alternate bars reach appeared at the expense of sinuous reaches, while
10
11 666 the meandering reaches were replaced by straight configurations; also in the tributaries the
12
13 667 increase of sinuous with alternate bars morphologies is visible. Although several large floods
14
15 668 occurred during the 1870s and the 1880s (Figure 9c), no appreciable widening trend is visible
16
17 669 between 1870 and 1905. Not even the extreme 1882 flood (Turri and Ruffo, 2005; probably
18
19 670 characterized by >100 yr recurrence interval in the main river and in many tributaries) had any
20
21 671 remarkable effect on the Adige channel morphology, already fixed by levees. The same 1882
22
23 672 event instead caused widening in the wider, uncontrolled Piave River (Comiti et al., 2011).
24
25 673 Between 1905 and 1917 (the “third phase”), narrowing reached maximum values in all reaches
26
27 674 (Figure 9) and channels were laterally stable, because channelization works were completed at
28
29 675 that time.

30
31
32 676 Recently, Marchese et al. (2017) analyzed the channel changes of 17 tributaries of the upper
33
34 677 Adige river basin from 1850s to 1950s, and found a net tendency – despite large intra- and inter-
35
36 678 catchment variability – for channel pattern simplification and narrowing mostly from 1850s to
37
38 679 1920s. Reaches of the Adige, located upstream the segment analyzed in this paper, suffered
39
40 680 narrowing between 1850s and 1920s and remained in equilibrium, or were interested by
41
42 681 narrowing or some widening between 1920s and 1950s. Final configuration was a pattern
43
44 682 simplification and a prevalent narrowing from 35% to 90 % in the entire period from 1850s to
45
46 683 1950s (Marchese et al., 2017). This tendency was attributed to climatic reasons (i.e. warmer and
47
48 684 drier period following the peak of the LIA, with less flood events and reduced sediment supply
49
50
51
52
53
54
55
56
57
58
59
60

1
2
3 685 from glaciers), in agreement with previous studies in larger rivers (Rumsby and Macklin, 1996;
4
5 686 Arnaud-Fassetta, 2003; Gob et al., 2008; Astrade et al., 2011). Forest cover expansion – and
6
7
8 687 thus a reduced sediment supply from hillslopes – had likely a minor or no role at all in the Adige
9
10 688 River (Marchese et al., 2017), given its limited magnitude (14% from 1855 to 1970, and thus
11
12 689 surely less until 1920s, Comiti, 2012), much lower compared to other Alpine basins in Italy and
13
14 690 France (Descroix and Gautier, 2002; Liébault and Piégay, 2002; Comiti et al., 2011).
15
16 691 Nonetheless, we argue that the channelization has largely prevailed over the climatic factors in
17
18 692 determining bar reduction and pattern change and in the main Adige River from early 1800s to
19
20 693 the early 20th century, and the results of the models on the role of channel width in bar formation
21
22 694 seems to support such a conclusion. In addition, relevant differences are evident when comparing
23
24 695 the Adige's evolutionary trajectory with those determined for the Tagliamento (Ziliani and
25
26 696 Surian, 2012) and Piave rivers (Comiti et al., 2011), which drain similar large basins (>2000
27
28 697 km²) in the Eastern Italian Alps – and thus share similar climatic variations – but were not
29
30 698 affected by channelization works in the 19th century. In fact, the Tagliamento and Piave rivers
31
32 699 were affected by limited channel width variations (not exceeding 7%) in this period,
33
34 700 notwithstanding a much more substantial basin land use change (i.e. natural afforestation due to
35
36 701 agricultural abandonment since the end of the 19th century) than in the Adige catchment (Tasser
37
38 702 et al., 2007).
39
40
41
42
43
44
45
46
47

48 704 *Channelization of large Alpine rivers: the Adige in a broader perspective*

49
50 705 Channelization of large Alpine rivers occurred systematically in the 19th century in almost all
51
52 706 Alpine countries. Table 5 synthesizes the relevant information on observable morphological
53
54 707 changes for six major large Alpine rivers located in 5 different countries (France, Switzerland,
55
56
57
58
59
60

1
2
3 708 Liechtenstein, Austria, Italy). Table 5 also reports available reach-averaged values of streamflow
4
5 709 Q , longitudinal slope S , channel width W , and sediment size D_{50} needed as input for the bar and
6
7
8 710 pattern predictors, together with the resulting values of the width to depth ratio β and of its
9
10 711 threshold for free bars formation β_c .

11
12
13 712 While embankments almost prevent any lateral planform change, still one morphological “degree
14
15 713 of freedom” is left in channelized rivers in terms of the development of bars within the levees.

16
17
18 714 While in the Rhone, Inn and Drau, like in the Adige, almost no bars can be observed at present
19
20 715 (e.g. references in Table 5, and Figure 6c and 6g); the Alpine Rhine and the Isère reacted in a
21
22 716 completely different way to channelization, developing regular sequences of alternate bars along
23
24
25 717 tens of river kilometers (Jäggi, 1984, Vautier, 2000, Jaballah et al., 2015, Jourdain et al., 2016,
26
27 718 Adami et al., 2016), thus suggesting a pronounced divergence of the related evolutionary
28
29 719 trajectories (Figure 10).

30
31
32 720 The application of the free-bar predictor (Colombini et al., 1987) to the Adige, the Drau, the
33
34 721 Upper Rhone, the Inn, the Alpine Rhine and the Isère offers a reliable explanation of such
35
36 722 diverging trajectories. In the Alpine Rhine and in the Isère, the difference $\beta - \beta_c$, which
37
38 723 measures the morphodynamic instability of the river bed, is always positive within a broad range
39
40 724 of bar-forming discharge values, implying bar formation (Figure 10b and 10c), as observed
41
42
43 725 (Adami et al., 2016, Serlet et al., 2017). In contrast, together with outcomes from the Drau, the
44
45 726 results of the present work (Figure 8 and Figure 10b and 10c) indicate that for most of its length,
46
47
48 727 the study segment of the Adige is characterized by a reach-averaged width to depth ratio β
49
50 728 smaller than the critical value β_c for bar formation. The Inn and the Rhone fall closer to the
51
52 729 theoretical threshold. The free-bar predictor can also be used to predict the minimum channel
53
54
55 730 width necessary to develop bars. The predicted ranges of such minimum width are 75-95 m for
56
57
58
59
60

1
2
3 731 macro-reach M4, 88-108 m for M5 and 91-111 m for M6, instead of the actual 65 m, 75 m and
4
5
6 732 70 m, respectively, and considering bar-forming discharges between Q_2 and Q_{10} . On average, the
7
8 733 application of the free-bar predictor suggests that the designed width of the channelized Adige is
9
10 734 approximately 20 m below the threshold for bar formation, which would have led to a
11
12 735 completely different fluvial landscape (e.g. Figure 10), and possibly management history, in the
13
14
15 736 last century.

16
17 737 The above comparison indicates the diversity of the morphological responses of these gravel-bed
18
19
20 738 rivers to channelization and how this is sensitive to the newly imposed channel width, or, more
21
22 739 precisely, width to depth ratio. Figure 10 conceptually summarizes the lessons learned from the
23
24 740 analysis performed on the Adige in the present work and attempts to provide a more general
25
26
27 741 illustration of gravel-bed river response to channelization, also based on the comparison reported
28
29 742 in Table 5 and integrating existing theoretical and observational knowledge.

30
31 743 Figure 10a shows the example of the Adige River, which was characterized by repetitive
32
33
34 744 downstream sequences of different planform morphologies before channelization, induced by
35
36 745 tributary confluences. The upper panel shows the qualitative downstream trend of the channel
37
38 746 width (or, equivalently, width to depth ratio under bar-forming conditions). The lower horizontal
39
40
41 747 dashed line refers to the threshold setting the transitions between a flat bed configuration (n. 1 in
42
43 748 panel b) and a bed morphology with free alternate bars (n. 2 in panel b). After channelization, the
44
45
46 749 morphology of the Adige, as well as of the Drau, mainly evolved into a flat-bed configuration
47
48 750 (n.1 in panel b), while the Isère and the Rhine fell above the threshold for free alternate bars, thus
49
50 751 displaying a similar configuration to n.2. Should channelization result into much higher values of
51
52
53 752 the width to depth ratio, the response of the bed morphology may increase in spatial complexity,
54
55 753 from alternate bars to low-flow braiding/ wandering, as illustrated by morphology n.3 in b).

1
2
3 754 Though not examined in detail in the present work, all the three bars and pattern predictors
4
5 755 indicate that this occurs when a second, higher transition range of the width to depth ratio is
6
7
8 756 crossed, as illustrated by the higher horizontal dashed line in a), which sets the transition
9
10
11 757 between morphologies n.2 and n.3 in b). Three actual examples of the possible responses to
12
13 758 channelization (n. 1, 2 and 3) taken from real-world channelized rivers are shown in Figure 10c.
14

15 759

16 760

17 18 19 20 761 **Conclusions**

21
22 762 Many large rivers in Europe underwent heavy modifications for land reclamation and flood
23
24 763 mitigation through centuries. As a consequence, the study of pre-alteration morphological
25
26
27 764 patterns and the related channel evolution following anthropic modifications is rather
28
29 765 challenging. This study provides a novel contribution for the understanding of Alpine river
30
31
32 766 dynamics because it deals with a different system compared to those already analyzed in the
33
34 767 literature and it integrates different approaches (i.e. reconstruction of evolutionary trajectory by
35
36 768 using historical maps; analytical model for free-bar prediction; channel pattern predictors).

37
38
39 769 Before the massive channelization, at the beginning of the 19th century, the Adige presented a
40
41 770 prevalence of single-thread patterns, except for reaches downstream of the main confluences,
42
43 771 which showed multi-thread morphologies. Channelization, between the 19th century and the
44
45
46 772 beginning of the 20th, caused channel morphology simplification and narrowing. Simultaneously,
47
48 773 a large proportion of bars and islands disappeared, not only because of the decrease of sediment
49
50
51 774 delivery, but mostly because of the new channel widths imposed by channelization works. The
52
53 775 free-bar predictor indeed showed that before channelization, morphodynamic instability was
54
55 776 promoting the occurrence of free-bars in all reaches, regardless of their morphologies. The new
56
57
58
59
60

1
2
3 777 channel widths had completely modified the picture by reducing the width to depth ratio below
4
5 778 the instability threshold and, as a consequence, the tendency of the Adige to develop free bars.
6
7
8 779 The present study therefore suggests the potential of bar theories, and of analogous simplified
9
10 780 morphodynamic modelling, to gain insights in fluvial processes and predict hypothetical future
11
12 781 trajectories as well as threshold ranges of key parameters like the channel width, which may be
13
14 782 subject to modification in the future within flood protection or river restoration projects based on
15
16 783 the increasingly adopted strategy of “giving more room to the river”.
17
18 784 At the same time, the study provides novel insights into the morphological response of large
19
20 785 gravel-bed rivers to channelization, confirming that the analysis of evolutionary trajectories is
21
22 786 fundamental to understand morphological modifications and their control factors.
23
24
25
26
27 787
28

29 788 **Acknowledgements**

30
31 789 This study was funded by the Autonomous Province of Bolzano with the project: “ETSCH-2000:
32
33 790 Historical changes in channel morphology over 2 Millennia”.
34
35 791 Authors are grateful to the reviewers and to the editor whose comments and critical appraisals
36
37 792 significantly helped to improve the paper. The paper has benefitted from comments and
38
39 793 suggestions by Erik Mosselman.
40
41 794 The authors gratefully acknowledge Pierpaolo Macconi and Omar Formaggioni for the provided
42
43 795 maps and data on historical flood events; and Martino Salvaro, Stefano Pellegrini and Andrea
44
45 796 Grillo for the field measurements and data analysis.
46
47
48
49
50
51 797
52
53 798
54
55 799
56
57
58
59
60

1
2
3 8004
5 8016
7
8 802 **References**9
10 803

11
12 804 Adami L, Bertoldi W, Zolezzi G. 2016. Multidecadal dynamics of alternate bars in the Alpine
13 Rhine River. *Water Resources Research*. doi:10.1002/2015WR018228.
14
15 805

16
17
18 806 Adler S, Chimani B, Drechsel S, Fischer A, Haslinger K, Hiebl J, Marigo G, Meyer V, Resch G,
19 Rudolph J, Seiser B, Vergeiner J, Zingerle C. 2015. Il clima del Tirolo - Alto Adige -
20
21 807 Bellunese.
22
23 808

24
25
26 809 Arnaud-Fassetta G. 2003. River channel changes in the Rhone Delta (France) since the end of
27 the Little Ice Age: geomorphological adjustment to hydroclimatic change and natural
28
29 810 resource management. *Catena* 51: 141-172.
30
31 811

32
33 812

34
35 813 Astrade L, Jacob-Rousseau N, Bravard JP, Allignol F, Simac L. 2011. Detailed chronology of
36 mid-altitude fluvial system response to changing climate and societies at the end of the
37
38 814 Little Ice Age (Southwestern Alps and Cévennes, France). *Geomorphology*, 133 (1-2): 100-
39
40 815 116. doi : 10.1016/j.geomorph.2011.06.028.
41
42 816

43
44
45 817

46
47 818 Autorità di Bacino dell'Adige 1995. Verso il piano di Bacino dell'Adige: progetto preliminare
48 stralcio. Quaderno 2. (in Italian).
49
50 819

51
52 820

53
54 821 Bassetti M, Borsato A. 2005. Evoluzione geomorfologica della Bassa Valle dell'Adige
55 dall'Ultimo Massimo Glaciale: sintesi delle conoscenze e riferimenti ad aree limitrofe. *Studi*
56
57 822

- 1
2
3 823 Trentini di Scienze Natutali, Acta Geologica 82: 31-42.
4
5
6 824
7
8 825 Beechie TJ, Liermann M, Pollock MM, Baker S, Davies J. 2006. Channel pattern and river-
9
10 826 floodplain dynamics in forested mountain river systems. *Geomorphology* 78: 124-141.
11
12
13 827
14
15 828 Beechie TJ, Imaki H. 2014. Predicting natural channel patterns based on landscape and
16
17 829 geomorphic controls in the Columbia River basin, USA. *Water Resources Research* 50: 39-
18
19 830 57. doi:10.1002/2013WR013629
20
21
22 831
23
24 832 Benda L, Andras K, Miller D, Bigelow P. 2004. Confluence effect in rivers: Interactions of basin
25
26 833 scale, network geometry, and disturbance regimes. *Water resources research* 40, W05402.
27
28 834 DOI: 10.1029/2003WR002583, 2004
29
30
31 835
32
33
34 836 Benda L, Veldhuisen C, Black J. 2003. Debris flows as agents of morphological heterogeneity at
35
36 837 low-order confluences, Olympic Mountains, Washington, *Geological Society of America*
37
38 838 *Bulletin* 115: 1110-1121.
39
40
41 839
42
43
44 840 Bravard JP. 1989. La metamorphose des rivieres des Alpes francaises a la fin du Moyen-Age et a
45
46 841 l'epoque moderne. *Bull. Soc. Geogr. Liege* 25: 145-157.
47
48 842
49
50 843 Brunetti M, Buffoni L, Maugeri M, Nanni T. 2000. Precipitation intensity trends in northern
51
52 844 Italy. *International Journal of Climatology* 20: 1017-1031.
53
54
55 845
56
57
58
59
60

- 1
2
3 846 Brunetti M, Colacino M, Maugeri M, Nanni T. 2001. Trends in the daily intensity of
4
5
6 847 precipitation in Italy from 1951 to 1996. *International Journal of Climatology* 21: 299-316.
7
8 848
9
10 849 Brunetti M, Maugeri M, Nanni T, Auer I, Böhm R, Schöner W. 2006. Precipitation variability
11
12 850 and changes in the greater Alpine region over the 1800–2003 period. *Journal of*
13
14 851 *Geophysical Research*, 111: D11107, doi:10.1029/2005JD006674
15
16
17 852
18
19
20 853 Campana D, Marchese E, Theule JI, Comiti F. 2014. Channel degradation and restoration of an
21
22 854 Alpine river and related morphological changes. *Geomorphology* 221: 230-241.
23
24
25 855
26
27 856 Church M. 2002. Geomorphic thresholds in riverine landscapes. *Freshwater Biology* 47: 541-
28
29 857 557.
30
31
32 858
33
34 859 Chiogna G, Majone B, Paoli KC, Diamantini E, Stella E, Mallucci S, Lencioni V, Zandonai F,
35
36 860 Bellin A. 2016. A review of hydrological and chemical stressors in the Adige catchment and
37
38 861 its ecological status. *Science of the Total Environment* 540: 429-443.
39
40
41
42 862 Colombini M, Seminara G, Tubino M. 1987. Finite-amplitude alternate bars. *Journal of Fluid*
43
44 863 *Mechanics* 181: 213-232.
45
46
47 864 Comiti F. 2012. How natural are Alpine mountain rivers? Evidence from the Italian Alps. *Earth*
48
49 865 *Surface Processes and Landforms* 37:693–707.
50
51
52 866
53
54
55 867 Comiti F, Da Canal M, Surian N, Mao L, Picco L, Lenzi MA. 2011. Channel adjustments and
56
57 868 vegetation cover dynamics in a large gravel bed river over the last 200 years.
58
59
60

1
2
3 869 Geomorphology 125: 147-159.

4
5 870

6
7
8 871 Crosato A, Mosselman E. 2009. Simple physics-based predictor for the number of river bars and
9
10 872 the transition between meandering and braiding. *Water Resources Research* 45: W03424,
11
12 873 DOI:10.1029/2008WR007242.

13
14
15 874

16
17
18 875 David M, Labenne A, Carozza JM, Valette P. 2016. Evolutionary trajectory of channel
19
20 876 planforms in the middle Garonne River (Toulouse SW France) over a 130-year period:
21
22 877 contribution of mixed multiple factor analysis (MFAmix). *Geomorphology* 258: 21-39.
23
24 878 DOI: [DOI: 10.1016/j.geomorph.2016.01.012](https://doi.org/10.1016/j.geomorph.2016.01.012).

25
26 879

27
28
29
30 880 Davies T, Campbell B, Hall B, Gomez C. 2013. Recent behavior and sustainable future
31
32 881 management of the Waiho River, Westland, New Zealand. *Journal of Hydrology* 52: 41-56.

33
34 882

35
36
37 883 Descroix L, Gautier E. 2002. Water erosion in the southern French Alps: climatic and human
38
39 884 mechanisms. *Catena* 50: 53–85. DOI:10.1016/S0341-8162(02)00068-1

40
41 885

42
43
44 886 Eaton BC, Millar RG, Davidson S. 2010. Channel patterns: Braided, anabranching, and single-
45
46 887 thread. *Geomorphology* 120(3-4): 353-364.

47
48
49 888 Frings RM, Ottevanger W, Sloff K. 2011. Downstream fining processes in sandy lowland rivers.
50
51 889 *Journal of Hydraulic Research* 49(2): 178- 193.

52
53
54
55 890 Fischer A, Seiser B, Stocker Waldhuber M, Mitterer C, Abermann J. 2015. Tracing glacier
56
57 891 changes in Austria from the Little Ice Age to the present using a lidar-based high-resolution

- 1
2
3 892 glacier inventory in Austria. *The Cryosphere* 9: 753-766. DOI: 10.5194/tc-9-753-2015
4
5
6 893
7
8 894 Fuganti A, Bazzoli G, Morteani G. 1996. The Quaternary evolution of the Adige Valley near the
9
10 895 city of Trento (Northern Italy) as deduced from wells and radiocarbon dating. Preliminary
11
12 896 results. *Studi Trentini di Scienze Naturali, Acta Geologica* 73 : 93-97.
13
14
15 897
16
17 898 Garcia Lugo G A, Bertoldi W, Henshaw A J, Gurnell AM. 2015. The effect of lateral
18
19 899 confinement on gravel bed river morphology. *Water Resour. Res.* 51: 7145- 7158. DOI
20
21 :10.1002/ 2015WR017081.
22 900
23 901
24
25
26 902 Gob F, Jacob N, Bravard JP, Petit F. 2008. The value of lichenometry and historical archives in
27
28 903 assessing the incision of submediterranean rivers from the Little Ice Age in the Ardèche and
29
30 904 upper Loire (France). *Geomorphology* 94: 170–183. DOI:10.1016/j.geomorph.2007.05.005
31
32 905
33
34
35 906 Grove JM. 2004. *Little Ice Ages: Ancient and Modern*, Routledge: London.
36
37 907
38
39
40 908 Hohensinner S, Habersack H, Jungwirth M, Zauner G. 2004. Reconstruction of the
41
42 909 characteristics of a natural alluvial river-floodplain system and hydromorphological changes
43
44 910 following human modifications: the Danube River (1812–1991). *River Research and*
45
46 911 *Applications* 20:25-41.
47
48 912
49
50
51 913 Hohensinner S, Sonnlechner C, Schmid M, Winiwarter V. 2013a. Two steps back, one step
52
53 914 forward: reconstructing the dynamic Danube riverscape under human influence in Vienna.
54
55
56
57
58
59
60

- 1
2
3 915 Water History 5: 121- 143.
4
5
6 916
7
8 917 Hohensinner S, Lager B, Sonnlechner C, Haidvogel G, Gierlinger S, Schmid M, Krausmann F,
9
10 918 Winiwarter V. 2013b. Changes in water and land: the reconstructed Viennese riverscape
11
12 919 from 1500 to the present. Water History 5: 145-172
13
14
15 920
16
17 921 Jaballah M, Camenen B, Pénard L, Paquier A. 2015. Alternate bar development in an alpine river
18
19 922 following engineering works. Advances in Water Resources 81:103–113.
20
21
22 923
23
24 924 Jäggi M. 1984. Formation and effects of alternate bars. Journal of Hydraulic Engineering 110
25
26 925 (2): 142–156. doi:10.1061/(ASCE) 0733-9429(1984)110:2(142).
27
28
29
30 926 Jourdain C, Belleudy P, Tal M, Malavoi JR. 2016. Mechanisms of vegetation removal by floods
31
32 927 on bars of a heavily managed gravel bed river (The Isere River, France). In EGU General
33
34 928 Assembly Conference Abstracts 18: 8111.
35
36
37 929 Klösch M, Habersack H. 2016. The Hydromorphological Evaluation Tool (HYMET).
38
39 930 Geomorphology, 291: 143-158. DOI: 10.1016/j.geomorph.2016.06.005
40
41
42
43 931
44
45 932 Liébault F, Piégay H. 2002. Causes of 20th century channel narrowing in mountain and piedmont rivers
46
47 933 of southeastern France. Earth Surface Processes and Landforms 27: 425-444.
48
49
50 934 Marchetti M. 2002. Environmental changes in the central Po Plain (northern Italy) due to fluvial
51
52 935 modifications and anthropogenic activities. Geomorphology 44: 361-373.
53
54
55 936 Marchese E, Scorpio V, Fuller I, McColl S, Comiti F. 2017. Morphological changes in Alpine
56
57
58
59
60

- 1
2
3 937 rivers following the end of the Little Ice Age. *Geomorphology* 295: 811-826. DOI:
4
5
6 938 10.1016/j.geomorph.2017.07.018
7
8
9 939 Mastrorunzio M, Dai Prà E. 2016a. Who needs Mitteleuropa old maps? Present-day applications
10
11 940 of Habsburg cartographic heritage. In: *Progress in Cartography*. Gartner G, Jobst M, Huang H
12
13 941 (eds.). Springer Verlag (Lecture Notes in Geoinformation and Cartography), Berlin:305-318.
14
15
16 942 Mastrorunzio M, Dai Prà E. 2016b. Editing historical maps: comparative cartography using
17
18 943 maps as tools. *E-Perimtron* 11 (4):183-195.
19
20
21 944
22
23 945 Meyer-Peter E, Hoeck E, Müller R. 1937. Die internationale Rheinregulierung von der
24
25 946 Illmündung bis zum Bodensee, *Schweizer Bauzeitung* Bd . 109 , Nr. 16 bis 18 , April/Mai
26
27
28 947
29
30 948 Millar RG. 2005. Theoretical regime equations for mobile gravel-bed rivers with stable banks.
31
32 949 *Geomorphology* 64: 207-220.
33
34
35
36 950 Moretto J, Rigon E, Mao L, Picco L, Delai F, Lenzi AM. 2014. Channel adjustments and island
37
38 951 dynamics in the Brenta River (Italy) over the last 30 years. *River Research and Applications*
39
40 952 30: 719-732. [DOI: 10.1002/rra.2676](https://doi.org/10.1002/rra.2676).
41
42
43
44 953 Petts GE. 1989. Historical analysis of fluvial hydrosystems. In: *Historical Change of Large*
45
46 954 *Alluvial Rivers: Western Europe*. GE Petts (Ed). J. Wiley & Sons:1-18.
47
48 955
49
50
51 956 Provansal M, Dufour S, Sabatie, F, Anthony EJ, Raccasi G, Robresco S. 2014. The geomorphic
52
53 957 evolution and sediment balance of the lower Rhône River (southern France) over the last
54
55 958 130 years: Hydropower dams versus other control factors. *Geomorphology* 219: 27-41.
56
57
58
59
60

- 1
2
3 959
4
5
6 960 Rice S, Church M. 1998. Grain size along two gravel-bed rivers: Statistical variation, spatial
7
8 961 pattern and sedimentary links. *Earth Surface Processes and Landforms* 23: 345-363.
9
10 962
11
12
13 963 Rinaldi M, Surian N, Comiti F, Bussettini M. 2013. A method for the assessment and analysis of
14
15 964 the hydromorphological condition of Italian streams: the Morphological Quality Index
16
17 965 (MQI). *Geomorphology* 180-181: 96-108.
18
19
20 966
21
22 967 Rinaldi M, Surian N, Comiti F, Bussettini M. 2015a. A methodological framework for
23
24 968 hydromorphological assessment, analysis and monitoring (IDRAIM) aimed at promoting
25
26 969 integrated river management. *Geomorphology* 251: 122-136. DOI:
27
28 970 [10.1016/j.geomorph.2015.05.010](https://doi.org/10.1016/j.geomorph.2015.05.010)
29
30
31 971
32
33
34 972 Rinaldi M, Gurnell AM, Belletti B, Berga Cano MI, Bizzi, Bussettini M, Gonzalez del Tanago
35
36 973 M, Grabowski R, Habersack R, Klösch M, Magdaleno Mas F, Mosselman E, Toro Velasco
37
38 974 M, Vezza P. 2015b. Final report on methods, models, tools to assess the hydromorphology
39
40 975 of rivers, Deliverable 6.2, Part 1, of REFORM (REstoring rivers FOR effective catchment
41
42 976 Management), a Collaborative project (large-scale integrating project) funded by the
43
44 977 European Commission within the 7th Framework Programme under Grant Agreement
45
46 978 282656.
47
48
49
50 979
51
52
53 980 Robl J, Hergarten S, Stüwe K. 2008. Morphological analysis of the drainage system in the
54
55 981 Eastern Alps. *Tectonophysics* 460: 263-277.
56
57
58
59
60

- 1
2
3 982
4
5
6 983 Rumsby BT, Macklin MG. 1996. Channel and floodplain response to recent abrupt climate
7
8 984 changes: the Tyne basin, northern England. *Earth Surface Processes and Landforms* 19:
9
10 985 499-515.
11
12 986
13
14
15 987 Schumm SA 1985. Patterns of alluvial rivers, *Annual Reviews Earth Planetary Sciences* 13: 5-
16
17 988 27.
18
19
20 989
21
22 990 Scorpio V, Aucelli PPC, Giano I, Pisano L, Robustelli G, Roskopf CM, Schiattarella M. 2015.
23
24 991 River channel adjustment in Southern Italy over the past 150 years and implications for
25
26 992 channel recovery. *Geomorphology* 251: 77-90. DOI: [DOI:](https://doi.org/10.1016/j.geomorph.2015.07.008)
27
28 993 [10.1016/j.geomorph.2015.07.008](https://doi.org/10.1016/j.geomorph.2015.07.008).
29
30 994
31
32
33
34 995 Scorpio V, Roskopf CM. 2016. Channel adjustments in a Mediterranean river over the last 150
35
36 996 years in the context of anthropic and natural controls. *Geomorphology* 275: 90-104. DOI:
37
38 997 [10.1016/j.geomorph.2016.09.017](https://doi.org/10.1016/j.geomorph.2016.09.017)
39
40 998
41
42
43 999 Siviglia A, Repetto R, Zolezzi G, Tubino M. 2008. River bed evolution due to channel
44
45 1000 expansion: general behaviour and application to a case study (Kugart River, Kyrgyz
46
47 1001 Republic). *River Research and Applications* 24: 1271-1287.
48
49 1002
50
51
52
53 1003 Stäuble S, Martin, Reynard E. 2008. Historical mapping for landscape reconstruction. In
54
55 1004 *Proceedings of the 6th ICA Mountain Cartography Workshop: Mountain Mapping and*
56
57
58
59
60

- 1
2
3 1005 Visualization. Institute of Cartography, ETH Zurich, Lenk, Switzerland (pp. 211-217).
4
5
6 1006
7
8 1007 Surian N, Rinaldi M. 2003. Morphological response to river engineering and management in
9
10 1008 alluvial channels in Italy. *Geomorphology* 50: 307–326.
11
12
13 1009
14
15 1010 Surian N, Rinaldi M, Pellegrini L, Audisio C, Maraga F, Teruggi L, Ziliani L. 2009a. Channel
16
17 1011 adjustments in northern and central Italy over the last 200 years. *Geol. Soc. Am. Spec. Pap.*
18
19 1012 451, 83–95.
20
21
22 1013
23
24 1014 Surian N, Ziliani L, Comiti F, Lenzi MA, Mao L. 2009b. Channel adjustments and alteration of
25
26 1015 sediment fluxes in gravel-bed rivers of North-Eastern Italy: potentials and limitations for
27
28 1016 channel recovery. *River Research and Applications* 25: 551-567.
29
30
31 1017
32
33 1018 Tasser E, Walde J, Tappeiner U, Teutsch A, Noggler W. 2007. Land-use changes and natural
34
35 1019 reforestation in the Eastern Central Alps. *Agriculture Ecosystems and Environment* 118:
36
37 1020 115-129.
38
39
40 1021
41
42 1022 Turri E, Ruffo S. 2005. *L'Adige, il fiume, gli uomini, la storia*. Cierre edizioni, Verona, 395.
43
44
45 1023
46
47 1024 VanUrk G, Smit. H. 1989. The lower Rhine: geomorphological changes. In: *Historical Changes*
48
49 1025 of Large Alluvial Rivers: Western Europe. GE Petts, Moller H, Roux AM (Eds). J Wiley &
50
51 1026 Sons, Chichester, England: 167-182.
52
53
54 1027
55
56
57
58
59
60

- 1
2
3 1028 Vautier F. 2000. Dynamique géomorphologique et végétalisation des cours d'eau endigués:
4
5 l'exemple de l'Isère dans le Grésivaudan. PhD Thesis, Université Grenoble 1, (in French).
6 1029
7
8 1030
9
10 1031 Vischer D. 1989. Impact of 18th and 19th century river training works: three case studies from
11
12 Switzerland. In: Historical Changes of Large Alluvial Rivers: Western Europe. GE Petts,
13 1032
14 Moller H, Roux AM (Eds). J Wiley & Sons, Chichester, England: 19-40.
15 1033
16
17 1034
18
19 1035 Wohl E. 2006. Human impacts to mountain streams. *Geomorphology* 79: 217–248.
20
21 1036
22
23 1037 Wyzga B. 1993. River response to channel regulation: case study of the Raba River, Carpathians,
24
25 Poland. *Earth Surface Processes and Landforms* 18: 541-556.
26 1038
27
28 1039
29
30 1040 Zawiejska J, Wyzga B. 2010. Twentieth-century channel change on the Dunajec River, southern
31
32 Poland: Patterns. *Geomorphology* 117: 234-246.
33 1041
34
35 1042
36
37 1043 Ziliani L, Surian N. 2012. Evolutionary trajectory of channel morphology and controlling factors
38
39 in a large gravel-bed river. *Geomorphology* 173-174: 104-117.
40 1044
41
42 1045
43
44 1046 Zolezzi G, Luchi R, Tubino M. 2009. Morphodynamic regime of gravel bed, single-thread
45
46 meandering rivers. *Journal of Geophysical Research* 114: F01005.
47 1047
48
49 1048 DOI:10.1029/2007JF000968.
50
51
52
53 1049
54
55 1050
56
57 1051
58
59
60

1
2
3 1052
4
5 1053
6
7 1054
8
9 1055
10 1056
11
12 1057
13
14 1058
15
16 1059
17
18 1060
19
20 1061
21 1062
22
23 1063
24 1064
25
26 1065
27
28 1066
29
30 1067
31
32 1068
33
34 1069
35 1070
36
37 1071
38
39 1072
40
41 1073
42 1074
43
44 1075

Table 1

Key features of historical maps dataset

Year	Title	Author	Archive	Scale	Number of georeferenced maps	RMSE (m)
1803-1805	Oeconomische Karte des Etschstromes und der umligenden Gegend in der Grafschaft Tirol [...] (<i>alias</i> : Nowack-Plan)	Nowack	TLA	1:3,456	131	1-9
1816-1821	Zweite Militär-Landesaufnahme (Franzische Landesaufnahme) (<i>alias</i> : Reininger-Geppert Karte)	Reininger-Geppert/ KuK Militär-Geographisches Institut	KA	1:28,800	15	10-17

1847-1848	Karte der Etschregulierung in 14 Blättern von Meran bis Borghetto suedliche Rovereto	Claricini Dornpacher	TLMF	1:20,736	14	6-27
1856-1861	Cadastral map (Franzsiszeischer Kataster/Austrian Land Cadastre)	KuK Generaldirektion des Grundsteuerkatasters	PAT/South Tyrol	1:2,880	>300	1.5-4.5
1870-1871	Dritte Militär-Landesaufnahme (Franzisco-Josephinische Landesaufnahme/Neue Aufnahme)	KuK Militär- Geographisches Institut	BEV	1:25,000	14	10-17
1904-1912	Vierte Militär-Landesaufnahme (Präzisionsaufnahme)	KuK Militär- Geographisches Institut	BEV	1:25,000	14	10-21
1915-1927	IGM serie 25v (<i>alias</i> : "Tavolette")	IGM (Istituto Geografico Militare)	UniTN	1:25,000	24	10-13

1076

1077 List of acronyms: RMSE = RMS error; TLA = Tiroler Landesarchiv (Innsbruck, Austria); KA =
 1078 Kriegsarchiv (Vienna, Austria); TLMF = Tiroler Landesmuseum Ferdinandeum (Innsbruck,
 1079 Austria); PAT: Cadastre Service, Autonomous Province of Trento (Italy); South Tyrol =
 1080 Cadastre Dept., Autonomous Province of Bolzano (Italy); BEV = Bundesamt für Eich- und
 1081 Vermessungswesen (Vienna, Austria); UniTN = Dept. of Humanities, University of Trento
 1082 (Italy)

1083

1084

1085

1086

1087 **Table 2**

1088

1089 Variables calculated from the digitized features, in 1803-1805

Variable	Symbol	Description
Average channel width	W	Ratio between the reach polygon area and its length (excluding islands)
Total average channel width	W_{tot}	Ratio between the reach polygon area and its length (including islands)
Bar ratio	B	Ratio between the area occupied by bars and the reach area
Island ratio	I	Ratio between the area occupied by the islands and the entire reach surface
Sinuosity index	SI	Ratio between the distance measured along the channel and the distance measured

1
2
3 along the valley bottom
4 Braiding index BI Average number of active channels separated by bars
5 Anastomosing index AI Average number of active channels separated by vegetated islands
6 Alluvial plain width AP Ratio between the valley polygon area and its length
7 Confinement index CI Ratio between the alluvial plain width and the channel width (Rinaldi et al., 2013)
8 Distance from tributary T Channel length between the downstream vertex of the reach and the nearest upstream
9 tributary
10 Valley slope Sv Average valley slope computed from the present valley bottom elevation
11 Channel slope Sc Average channel slope computed from the present valley bottom elevation
12
13
14

15 1090

16 1091 First geodatabase detailing morphological pattern before channelization.

17 1092

18 1093

19 1094

20 1095

21 1096

22 1097

23 1098

24 1099

25 1100

26 1101

27 1102

28 1103

29 1104

30 1105

31 1106

32 1107 **Table 3**

33 1108 Parameters used for the bar and channel pattern predictors for the 6 macro-reaches

Macro-reach	W pre (m)	W post (m)	Sc (%)	D ₅₀ (mm)	Q ₂ (m ³ /s)	Q ₅ (m ³ /s)	Q ₁₀ (m ³ /s)	Q ₂₀ (m ³ /s)
1	202 ± 95	58 ± 12	0.3	10.5	219	298	350	402
2	81 ± 19	75 ± 11	0.081	10.5	219	298	350	402
3	137 ± 50	82 ± 9	0.18	6.05	581	757	874	1005
4	115 ± 16	64 ± 6	0.066	16.54	581	757	874	1005
5	149 ± 44	73 ± 20	0.093	13.2	769	1072	1272	1438

6 121 ± 18 69 ± 8 0.083 11.13 769 1072 1272 1438

1109

1110 W = channel width, pre- and post- channelization, Sc = channel slope, D₅₀ = median subsurface
 1111 grain size, Q₂, Q₅, Q₁₀, Q₂₀ = daily streamflow value with recurrence interval > 2, 5, 10 and 20
 1112 years.

1113

1114

1115

1116

1117

1118

1119

1120

1121

1122

1123

1124

1125

1126

1127

1128

1129

1130

1131

1132

1133 **Table 4**

1134 Minimum/Average/Maximum values of the morphological parameters (as reported in Table 2)
 1135 for the 4 homogeneous groups in the Adige River in 1803-1805

	Group 1	Group 2	Group 3	Group 4
W (m)	60/ 102/ 135	68/ 111/ 148	249/ 310/ 372	83/ 167/ 291
W_{tot} (m)	60/ 104/ 145	74/ 114/ 150	486/ 504/ 522	83/ 208/ 327
AP (m)	805/ 2085/ 3505	295/ 928/ 1598	1366/ 1674/ 1982	386/ 1178/ 2524

T (km)	5 / 17/ 37	2/ 12/ 40	0.5/ 5.5/ 10	0.5/ 4.5/ 11.7
S_v (%)	0.01/ 0.09/ 0.21	0.01/ 0.08/ 0.26	0.13/ 0.33/ 0.54	0.02/ 0.23/ 0.52
S_c (%)	0.01/ 0.08/ 0.18	0.01/ 0.06/ 0.18	0.12/ 0.32/ 0.53	0.01/ 0.21/ 0.5
B (m²/m²)	0.0/ 0.28/ 0.57	0.06/ 0.21/ 0.45	0.63/ 0.68/ 0.72	0.32/ 0.50/ 0.61
I (m²/m²)	0.0/ 0.02/ 0.24	0.0/ 0.03/ 0.28	0.31/ 0.7/ 1.1	0.0/ 0.23/ 0.84
SI	1.03/ 1.11/ 1.34	1.04/ 1.43/ 2.24	1.02/ 1.03/ 1.05	1.02/ 1.14/ 1.40
BI	1/ 1.13/ 1.67	1/ 1.08/ 1.36	2.64/ 3.68/ 4.71	1.29/ 1.94/ 3.50
AI	1/ 1.11/ 2.14	1/ 1.04/ 1.27	3/ 3.46/ 3.92	1.00/ 1.36/ 2.08
CI (m/m)	13.5/ 20. 5/ 35.1	2.6/ 8.1/ 13.2	3.7/ 5.8/ 8.0	1.9/ 7.7/ 18.52

1136

1137

1138

1139

1140

1141

1142

1143

1144

1145

1146

1147

1148

1149

1150

1151

1152

1153

1154 **Table 5**

1155 Morphological response of selected reaches of large Alpine rivers to massive channelization
 1156 works initiated in the 19th century and representative, reach-averaged hydro-morphological
 1157 conditions for the application of bar and pattern predictors.

1158

River name	Segment location: between	Pre-channelization morphology	Observable riverbed morphology under low	Q (m ³ /s)	S (%)	W (m) designed	D ₅₀ (mm)	β	β _c
------------	------------------------------	----------------------------------	---	--------------------------	----------	-------------------	-------------------------	---	----------------

flow conditions ⁽⁶⁾

Alpine Rhine (Switzerland, Liechtenstein, Austria)	Confluences with Landquart and Ill rivers	Wandering, anabranching ⁽¹⁾	Alternate bars, mostly non-vegetated ⁽⁷⁾	1600	0.2	95	40	24.9	21.7
Isere (France)	Albertville and Grenoble	Braided ⁽²⁾	Alternate bars, mostly vegetated ⁽²⁾	800	0.15	100	50	35.2	11.6
Rhone (Switzerland)	Sion and Martigny	Braided, anabranching ⁽³⁾	No bars	650	0.1	70	23	21	22.4
Drau (Austria)	Lienz and Villach	Anabranching, sinuous ⁽⁴⁾	No bars	570 ⁽⁴⁾	0.2	40	32	11.4	22.8
Inn (Austria)	Innsbruck and Kufstein	Sinuuous with bars ⁽⁵⁾	Few bars, not systematic	724	0.1	90	20	26.4	24.2
Adige / Etsch (Italy)	Trento and Rovereto	Sinuuous, anabranching, meandering	No bars	1200	0.09	70	11	15.4	29.3

1159

1160 Sources of information: ⁽¹⁾ Meyer-Peter et al. (1937); ⁽²⁾ Vautier (2000); ⁽³⁾ Stäuble et al. (2008);
 1161 ⁽⁴⁾, ⁽⁵⁾ Second Military Survey, www.mapire.eu, ; ⁽⁶⁾ Google Earth; ⁽⁷⁾ Adami et al. (2016); ⁽⁸⁾
 1162 Klosch and Habersack (2016).

1163

1164

1165

1166

1167

1168 **Captions**

1169 **Figure 1.** Location of the Adige River and of the analyzed tributaries. Codes for gauging
 1170 stations: 1 = Ponte Adige; 2 = Bronzolo; 3 = Trento. Catchments areas and total studied reaches
 1171 length in the tributaries : Passirio = 414 km², 2.2 km; Rio di Nova = 17.4 km², 2.6 km; Valsura
 1172 = 282.4 km², 2.9 km; Talvera = 418 km², 2.7 km ; Isarco = 4164.4 km², 6.6 km; Noce = 1366. 67
 1173 km², 6.4 km; Avisio = 940 km², 2.9 km; Fersina = 170 km², 2.9 km.

1174

1
2
3 1175 **Figure 2.** Examples of maps used in the multi-temporal analysis. Reaches number 2 and 3 (a),
4 1176 reaches number 7 and 8 (b), reach number 22 (c).
5
6
7 1177

8
9 1178 **Figure 3.** Statistical distribution for: channel width (a), total channel width (b), island ratio (c),
10 1179 bar ratio (d), alluvial plain width (e), confinement index (f), valley slope (g) and distance from
11 1180 the main upstream tributary (h), for the channel morphology types (42 reaches) in 1803-1805.
12 1181 Codes for channel patterns: B: braided; A: anabranching; W: wandering; SAB: sinuous with
13 1182 alternate bars; S: sinuous; M: meandering.
14
15
16 1183

17
18 1184 **Figure 4.** Results of the PCA on the 42 reaches of the Adige River, in 1803-1805 (a).
19 1185 Distribution of channel morphologies (b), and of homogeneous groups (c) for the 42 reaches and
20 1186 segmentation into six macro-reaches (M1-M6). Dashed lines indicate main tributaries.
21
22
23 1187

24
25 1188 **Figure 5.** Comparison of the patterns obtained by applying the hybrid-bar predictor (Crosato and
26 1189 Mosselman, 2009) and the channel pattern predictor (Eaton et al., 2010) with those observed in
27 1190 the 42 reaches, for both the configurations before (PRE) and after (POST) channelization.
28
29
30 1191

31
32 1192 **Figure 6.** Channel width changes (a, e); channel morphology distribution (b, f); bar ratio
33 1193 statistical distribution (c, g); island ratio statistical distribution (d, h) between 1803 and 1917, in
34 1194 multi-thread and single-thread macro-reaches. Codes for channel patterns as in Figure 3.
35
36
37 1195

38
39 1196 **Figure 7.** Univariate statistical distribution of tributaries channel width variation, here defined as
40 1197 the ratio between the channel width in a year and the channel width in 1803-1805 (a), bar ratio
41 1198 (b), bank work ratio (c), and channel morphology (d), between 1803-1805 and 1917. Codes for
42 1199 channel patterns as defined in Figure 3.
43
44
45 1200

46
47 1201 **Figure 8.** Results of the free-bar predictor applied to the 6 macro reaches. Positive values of the
48 1202 difference $\beta - \beta_c$ denote unstable channel bed, thus bar formation, while negative values are
49 1203 related to a flat channel bed. Blue filled circles refer to the pre channelization configuration with
50 1204 the present hydrology (Q_2 , Q_5 , Q_{10}), the red asterisks show the effect of increasing the discharge
51
52
53
54
55
56
57
58
59
60

1
2
3 1205 to the hypothesized LIA values (Q_5 , Q_{10} , Q_{20}), black open circles correspond to the post
4 1206 channelization conditions (using Q_2 , Q_5 , Q_{10}).
5
6
7 1207

8
9 1208 **Figure 9.** Channel width, bar ratio, and rectification works evolutionary trajectories between
10 1209 1803-1805 and 1917, for the Adige river (a) and for the tributaries (b). Yearly number of floods
11 1210 occurred in the Adige basin and in the main stem (c). Subscript 1803 indicates values observed
12 1211 on the Novak map.
13
14
15
16 1212

17 1213 **Figure 10.** Conceptual diagram of large gravel bed rivers response to channelization, inspired
18 1214 from the example of the Adige River. a) (Upper panel) Qualitative downstream trend of the
19 1215 unconfined channel width (equivalently, of the width to depth ratio under bar-forming
20 1216 conditions), and related downstream variability in channel morphology, with the discontinuity
21 1217 due to the inflow of a lateral tributary delivering high coarse sediment input. The horizontal
22 1218 dashed lines illustrate two threshold values that set the transitions between the corresponding
23 1219 morphologies 1, 2 and 3 sketched in panel (b). The lower panel of (a) shows an actual example
24 1220 of such downstream morphological variability observed in the Adige River downstream the
25 1221 confluence with the Isarco River (from Novack historical map, lower panel). c) Examples of
26 1222 channelized rivers showing different morphological responses to channelization: 1 Kugart River,
27 1223 near Jalal-Abad, Kyrgyz Republic (Siviglia et al., 2008); 2 Alpine Rhine close to Vaduz
28 1224 (Liechtenstein); 3 Adige near Auer/Ora in South Tyrol, Italy. Flow is from left to right. Source:
29 1225 Google Earth.
30
31
32
33
34
35
36
37
38
39
40
41 1226
42 1227
43
44
45
46
47
48
49
50
51
52
53
54
55
56
57
58
59
60

1
2
3
4
5
6
7
8
9
10
11
12
13
14
15
16
17
18
19
20
21
22
23
24
25
26
27
28
29
30
31
32
33
34
35
36
37
38
39
40
41
42
43
44
45
46
47
48
49
50
51
52
53
54
55
56
57
58
59
60

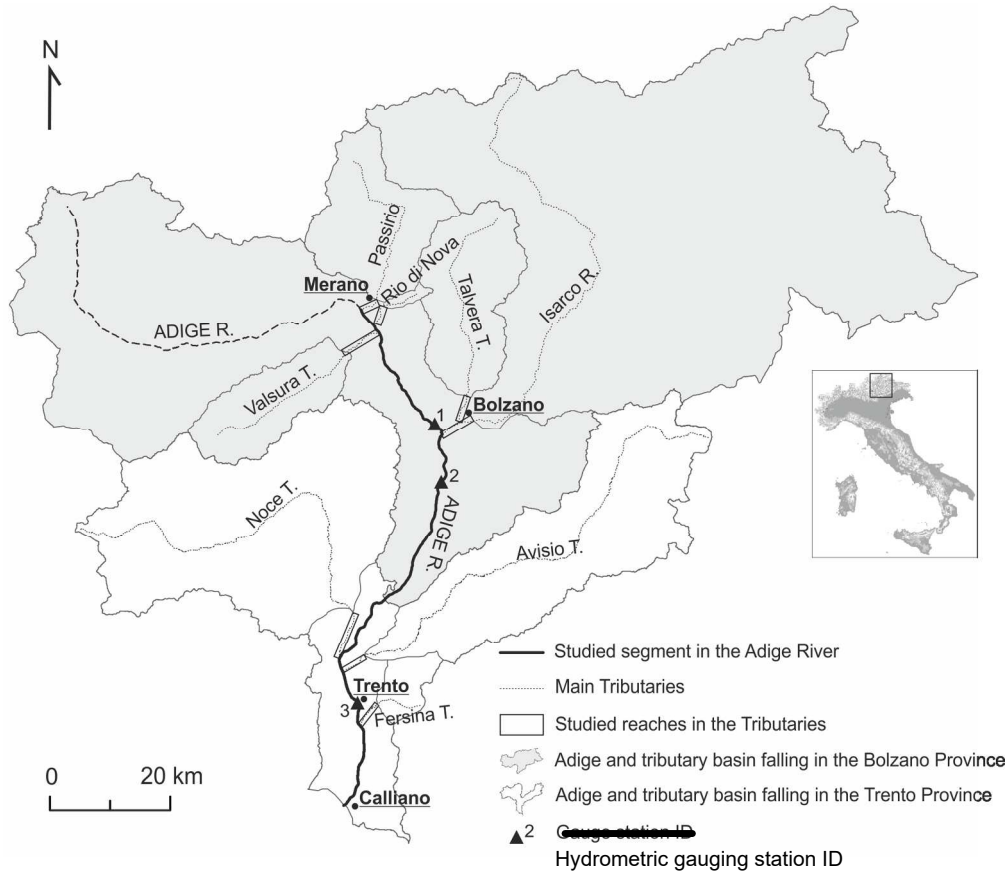


Figure 1. Location of the Adige River and of the analyzed tributaries. Codes for gauging stations: 1 = Ponte Adige; 2 = Bronzolo; 3 = Trento. Catchments areas and total studied reaches length in the tributaries : Passirio = 414 km², 2.2 km; Rio di Nova = 17.4 km², 2.6 km; Valsura = 282.4 km², 2.9 km; Talvera = 418 km², 2.7 km ; Isarco = 4164.4 km², 6.6 km; Noce = 1366. 67 km², 6.4 km; Avisio = 940 km², 2.9 km; Fersina = 170 km², 2.9 km.

174x149mm (300 x 300 DPI)



1
2
3
4
5
6
7
8
9
10
11
12
13
14
15
16
17
18
19
20
21
22
23
24
25
26
27
28
29
30
31
32
33
34
35
36
37
38
39
40
41
42
43
44
45
46
47
48
49
50
51
52
53
54
55
56
57
58
59
60

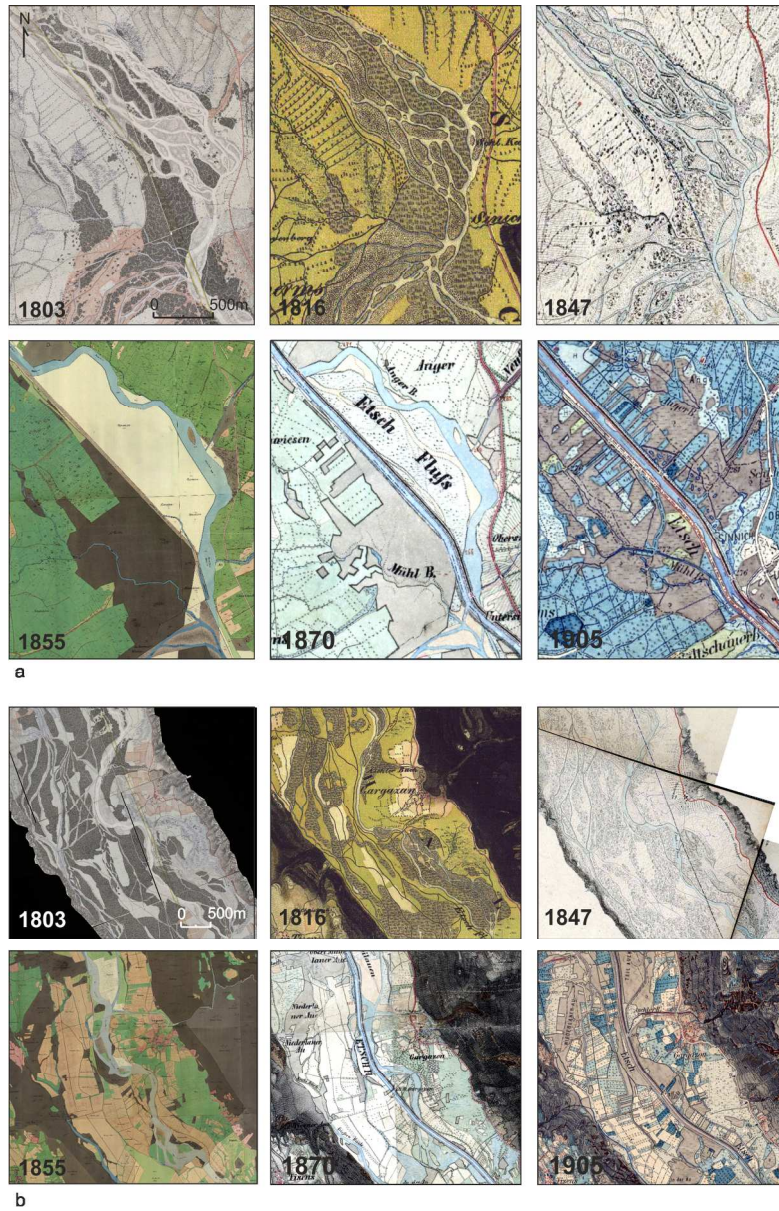


Figure 2. Examples of maps used in the multi-temporal analysis. Reaches number 2 and 3 (a), reaches number 7 and 8 (b), reach number 22 (c).

150x231mm (300 x 300 DPI)

1
2
3
4
5
6
7
8
9
10
11
12
13
14
15
16
17
18
19
20
21
22
23
24
25
26
27
28
29
30
31
32
33
34
35
36
37
38
39
40
41
42
43
44
45
46
47
48
49
50
51
52
53
54
55
56
57
58
59
60

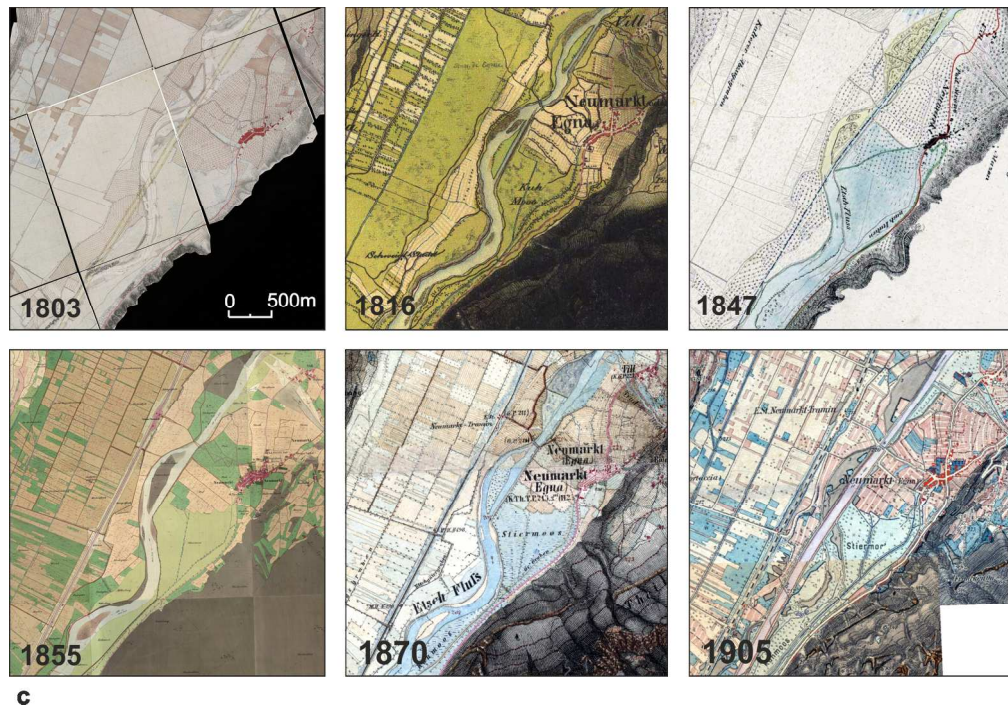


Figure 2. Examples of maps used in the multi-temporal analysis. Reaches number 2 and 3 (a), reaches number 7 and 8 (b), reach number 22 (c).

179x124mm (300 x 300 DPI)

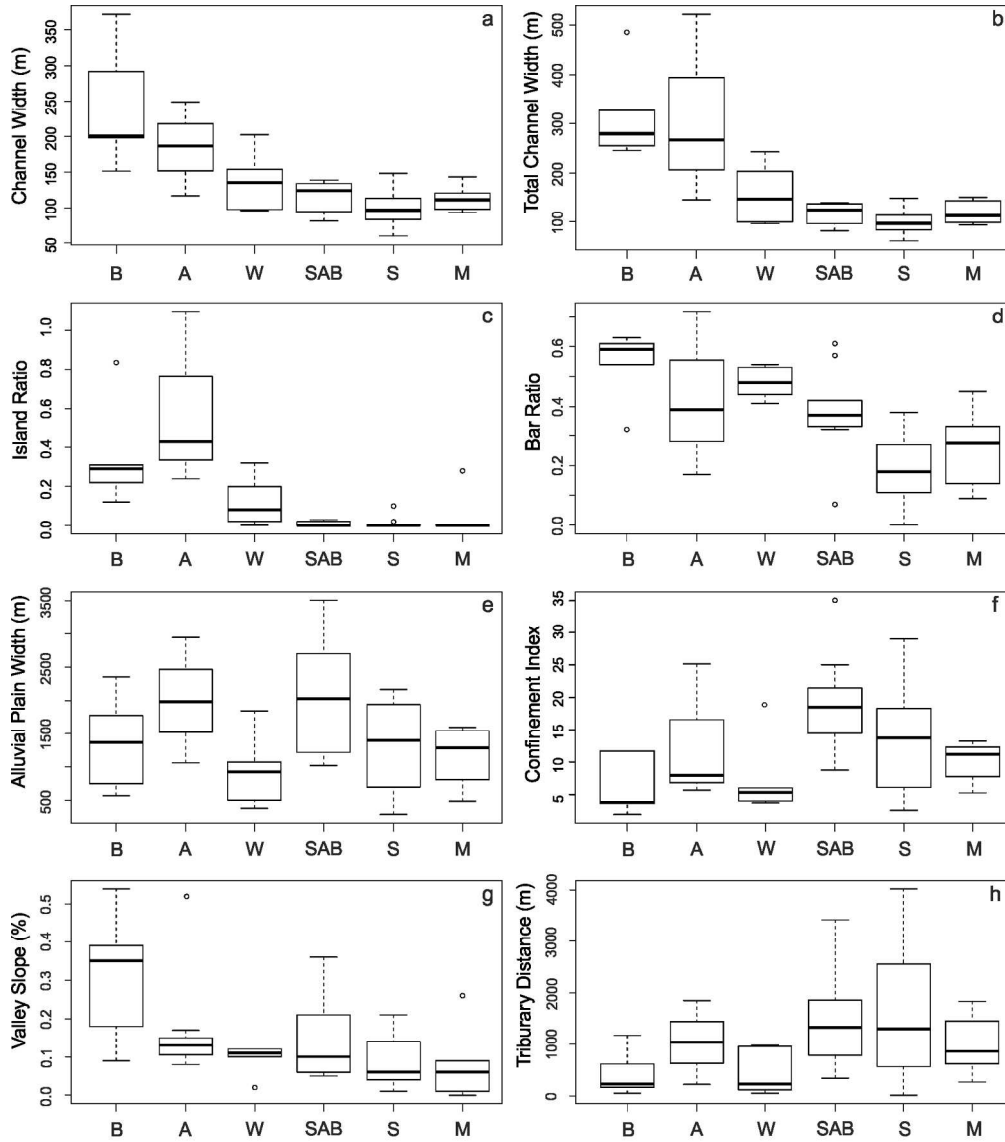


Figure 3. Statistical distribution for: channel width (a), total channel width (b), island ratio (c), bar ratio (d), alluvial plain width (e), confinement index (f), valley slope (g) and distance from the main upstream tributary (h), for the channel morphology types (42 reaches) in 1803-1805. Codes for channel patterns: B: braided; A: anabranching; W: wandering; SAB: sinuous with alternate bars; S: sinuous; M: meandering.

170x193mm (300 x 300 DPI)

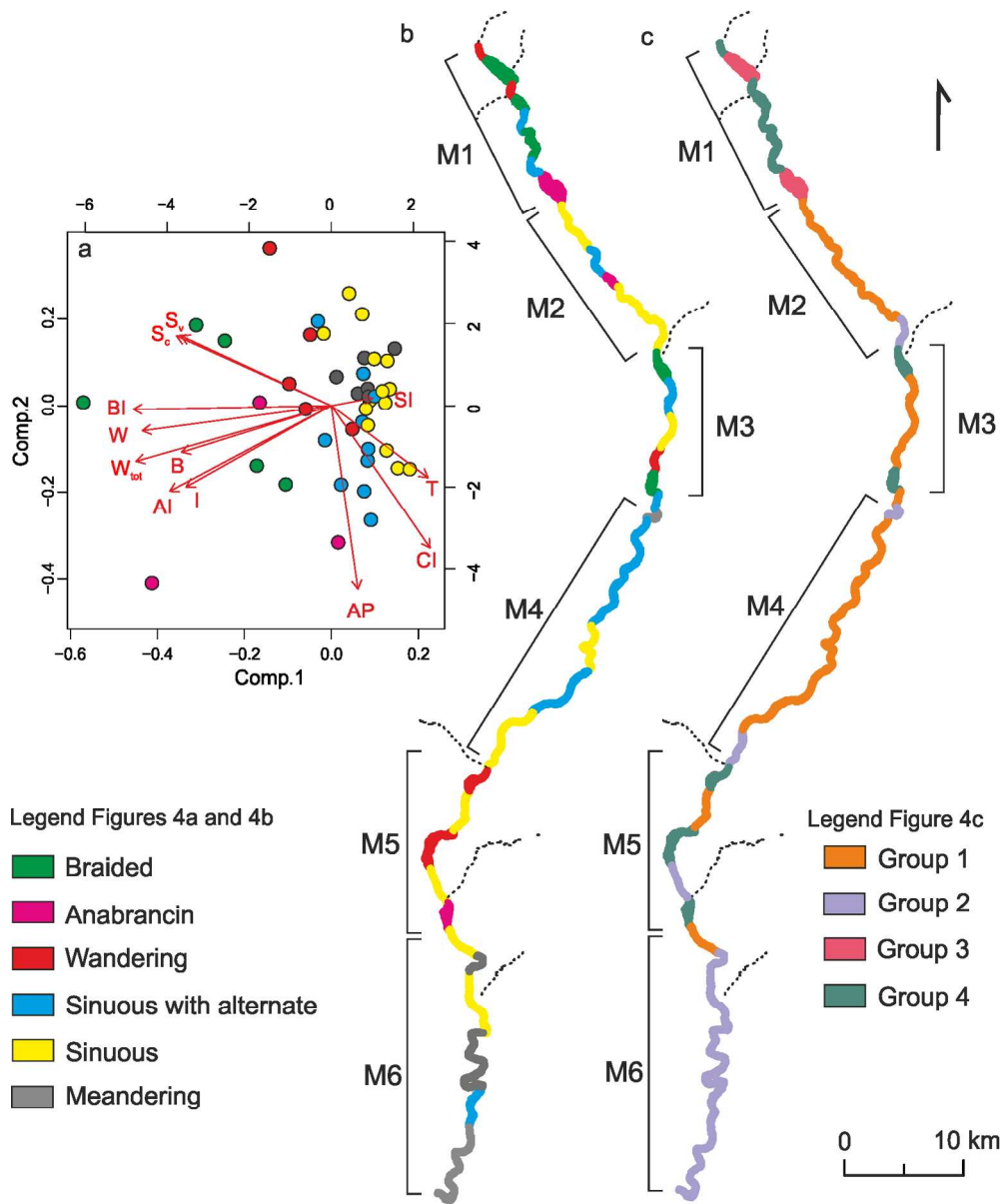


Figure 4. Results of the PCA on the 42 reaches of the Adige River, in 1803-1805 (a). Distribution of channel morphologies (b), and of homogeneous groups (c) for the 42 reaches and segmentation into six macro-reaches (M1-M6). Dashed lines indicate main tributaries.

152x181mm (300 x 300 DPI)

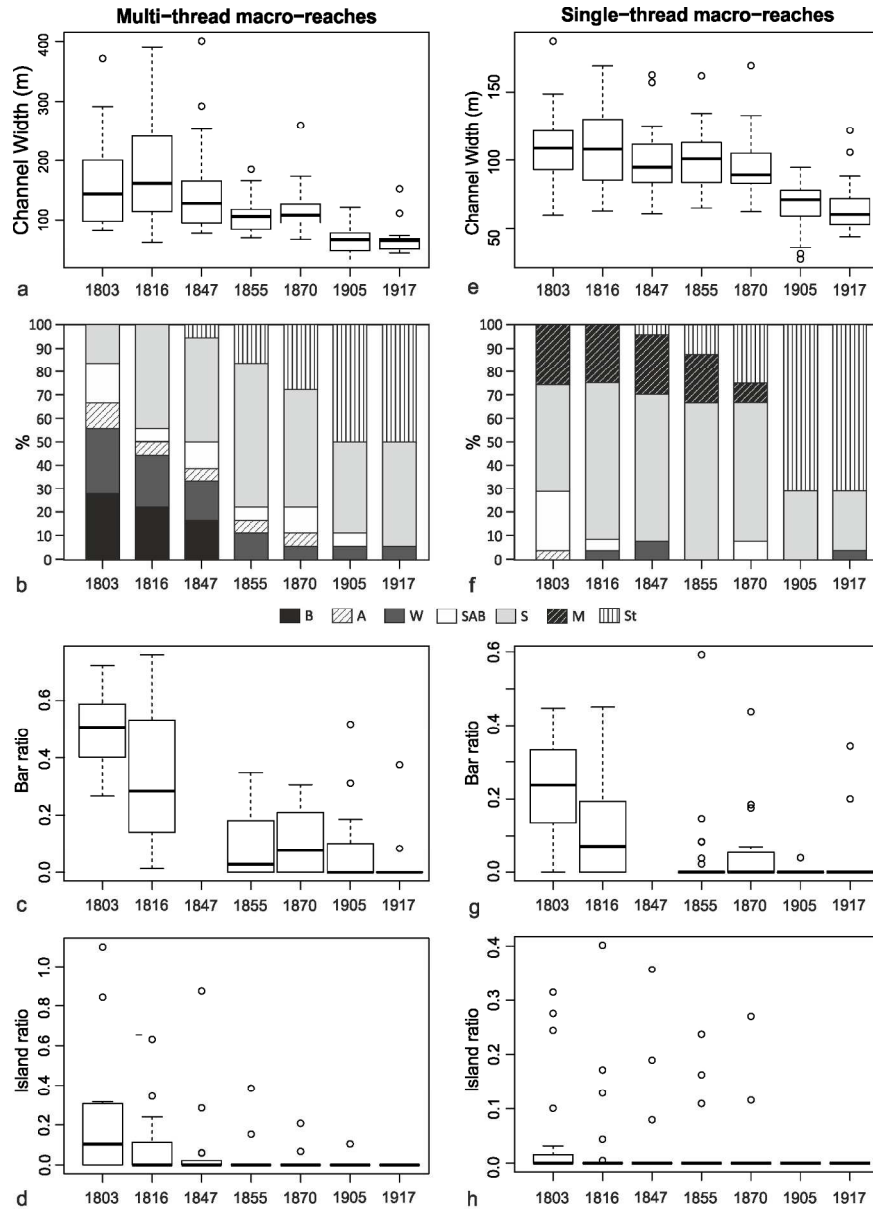


Figure 6. Channel width changes (a, e); channel morphology distribution (b, f); bar ratio statistical distribution (c, g); island ratio statistical distribution (d, h) between 1803 and 1917, in multi-thread and single-thread macro-reaches. Codes for channel patterns as in Figure 3.

160x221mm (300 x 300 DPI)

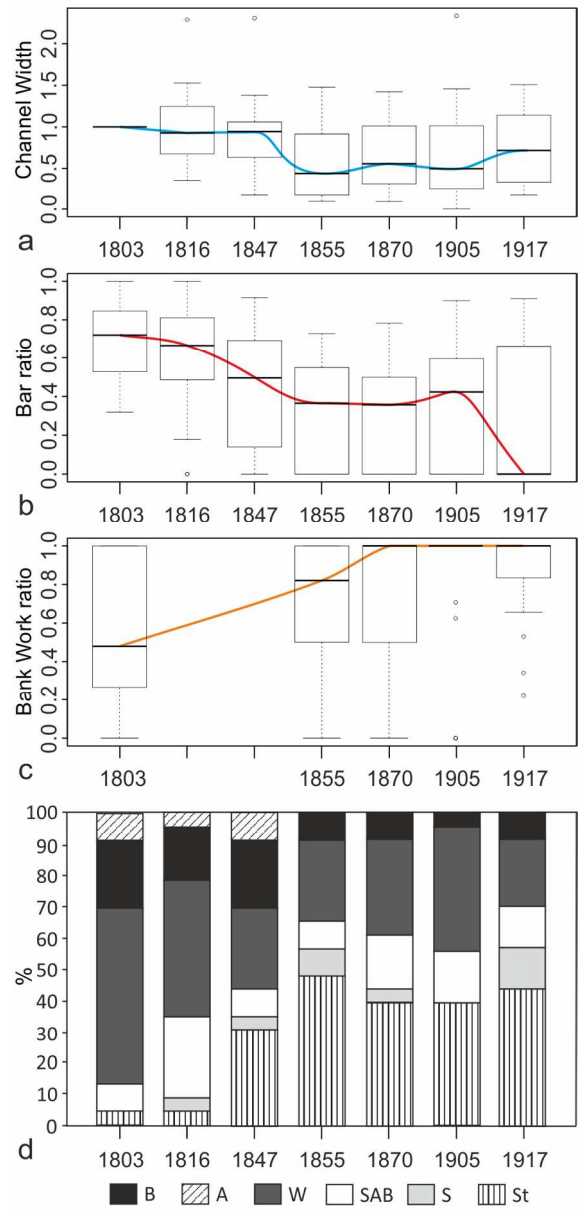
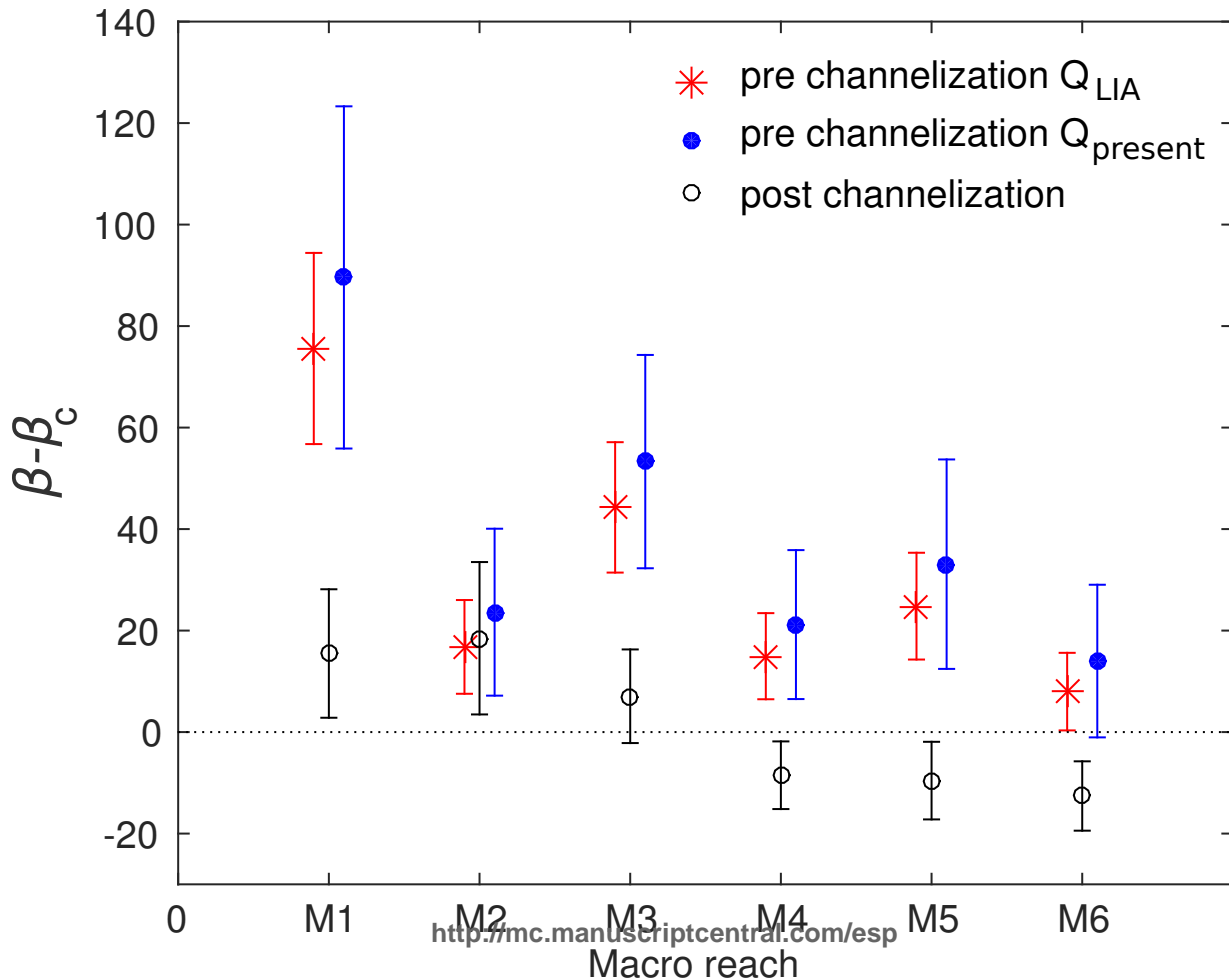


Figure 7. Univariate statistical distribution of tributaries channel width variation, here defined as the ratio between the channel width in a year and the channel width in 1803-1805 (a), bar ratio (b), bank work ratio (c), and channel morphology (d), between 1803-1805 and 1917. Codes for channel patterns as defined in Figure 3.

83x176mm (300 x 300 DPI)



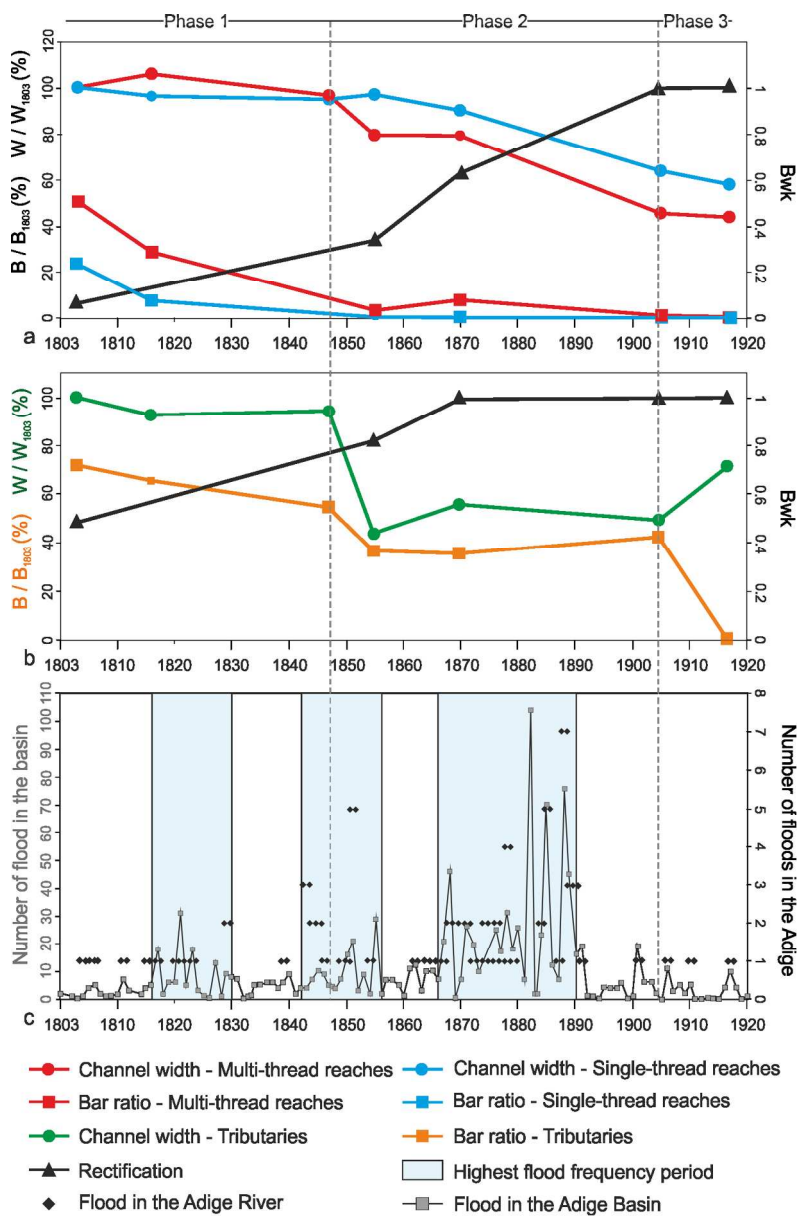


Figure 9. Channel width, bar ratio, and rectification works evolutionary trajectories between 1803-1805 and 1917, for the Adige river (a) and for the tributaries (b). Yearly number of floods occurred in the Adige basin and in the main stem (c). Subscript 1803 indicates values observed on the Novak map.

129x198mm (300 x 300 DPI)

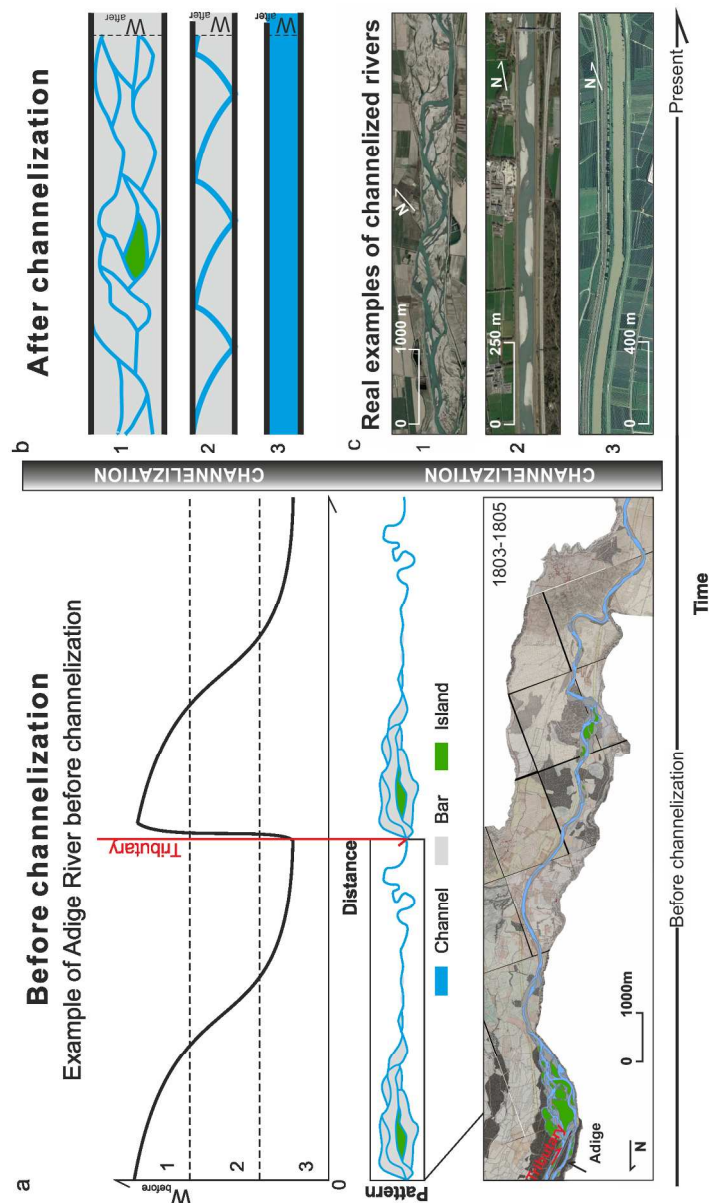


Figure 10. Conceptual diagram of large gravel bed rivers response to channelization, inspired from the example of the Adige River. a) (Upper panel) Qualitative downstream trend of the unconfined channel width (equivalently, of the width to depth ratio under bar-forming conditions), and related downstream variability in channel morphology, with the discontinuity due to the inflow of a lateral tributary delivering high coarse sediment input. The horizontal dashed lines illustrate two threshold values that set the transitions between the corresponding morphologies 1, 2 and 3 sketched in panel (b). The lower panel of (a) shows an actual example of such downstream morphological variability observed in the Adige River downstream the confluence with the Isarco River (from Novack historical map, lower panel). c) Examples of channelized rivers showing different morphological responses to channelization: 1 Kugart River, near Jalal-Abad, Kyrgyz Republic (Siviglia et al., 2008); 2 Alpine Rhine close to Vaduz (Liechtenstein); 3 Adige near Auer/Ora in South Tyrol, Italy. Flow is from left to right. Source: Google Earth.

135x230mm (300 x 300 DPI)

1
2
3
4
5
6
7
8
9
10
11
12
13
14
15
16
17
18
19
20
21
22
23
24
25
26
27
28
29
30
31
32
33
34
35
36
37
38
39
40
41
42
43
44
45
46
47
48
49
50
51
52
53
54
55
56
57
58
59
60

For Peer Review